EFFECTIVE SEALING AND MONITORING OF SMALL MOVEMENT EXPANSION JOINTS IN CONNECTICUT BRIDGES

March 2017

Ramesh B. Malla, Ph.D. (Principal Investigator)
Montgomery T. Shaw, Ph.D. (Co-Principal Investigator)
and
Dominic Kruszewski (Graduate Research Assistant)

JHR 17-329 Project 15-02

This research was sponsored by the Joint Highway Research Advisory Council (JHRAC) of the University of Connecticut and the Connecticut Department of Transportation and was performed through the Connecticut Transportation Institute of the University of Connecticut.

The contents of this report reflect the views of the authors who are responsible for the facts and accuracy of the data presented herein. The contents do not necessarily reflect the official views or policies of the University of Connecticut or the Connecticut Department of Transportation. This report does not constitute a standard, specification, or regulation.

Technical Report Documentation Page

1. Report No.	2. Government Accession No.	3. Recipient's Catalog No.
JHR 17-329	N/A	

4. Title and Subtitle	5. Report Date
Effective Sealing and Monitoring of Small Movement Expansion Joints in Connecticut Bridges	March 2017
	6. Performing Organization Code: CCTRP 15-02

7. Author(s)	8. Performing Organization Report No.
Ramesh B. Malla, Ph.D. (Principal Investigator), Montgomery T. Shaw, Ph.D. (Co-Principal Investigator), and Dominic Kruszewski (Graduate Research Assistant)	JHR 17-329

9. Performing Organization Name and Address	10. Work Unit No. (TRAIS)
University of Connecticut Connecticut Transportation Institute Storrs, CT 06269-5202	N/A
	11. Contract or Grant No.: N/A

12. Sponsoring Agency Name and Address	13. Type of Report and Period Covered
Connecticut Department of Transportation 2800 Berlin Turnpike Newington, CT 06111	Final
	14. Sponsoring Agency Code: CCTRP 15-02

15. Supplementary Notes

This study was conducted under the Connecticut Cooperative Transportation Research Program (CCTRP), http://www.cti.uconn.edu/cctrp/.

16. Abstract

One in nine bridges in the United States is rated as structurally deficient by the 2013 Infrastructure Report Card published by the American Society of Civil Engineers. One of the primary degradation factors that contribute to compromising the structural integrity of bridges involves leaking joints, which allow water, debris and deicing corrosive materials to penetrate below the deck and damage the substructure. Currently, poured silicone sealants must be replaced every 2-3 years in Connecticut mainly due to delamination of the sealant from the substrate. A novel silicone foam sealant has been previously developed at the University of Connecticut to provide a long term, cost-effective sealing method for small-movement expansion joints. This report summarizes the laboratory testing, field installation, and in-service monitoring of the novel foam sealant, with and without primer in bridges, including wider gap joints and higher traffic volume than used in the earlier studies. As part of the laboratory testing, tension and adhesion tests were conducted to examine the general mechanical behavior of the foam sealant under uniaxial tension. Additionally, an aging study was conducted to determine the performance of the foam and solid sealants when exposed to accelerated laboratory aging, salt exposure, and primer application. The results of these tests showed that the foam sealant performed better than the commercial solid sealant in adhesion to the substrate and reduced the modulus (stress at 100 percent strain), therefore, decreasing the stresses at the interaction surface). Next, the foam and solid sealants were installed on three in-service bridges in Connecticut to examine their performance in a real operating environment. During the 6-month monitoring period, in general, fewer failures were observed on the foam sealant than the commercial solid sealant.

17. Key Words	18. Distribution Statement
Bridges, structures, expansion joints, silicone sealant, foam sealant, traffic monitoring, thermal expansion, stress, strain, aging, salt effect	No restrictions. This document is available to the public through the National Technical Information Service Springfield, Virginia 22161

19. Security Classif. (of this report)	20. Security Classif. (of this page)	21. No. of Pages	22. Price
Unclassified	Unclassified	77	N/A

ACKNOWLEDGEMENTS

The research team would like to thank all organizations and individuals, who have contributed to making this research possible. First of all, sincere thanks are due to the Connecticut Department of Transportation (CT DOT) and the State of Connecticut for the financial support. The research team acknowledges and deeply appreciates the support and advice from the following members of CT DOT:

(1) David Hiscox, Bradley Overturf, Anne-Marie McDonnell, Michael Connors, Richard C, Van Allen, and James Fallon, for coordinating requests by the research team and providing advice on the research project;
(2) Technical Advisory Committee (TAC) members, David Hiscox, Douglas Harz, Jeffrey Cheng, Matthew Carr, James Bedard, and James Mahoney for providing technical advice towards successful completion of this project;
(3) Seth Burgess, Awni Allamadani, and James Bedard for coordinating the field installation and logistical planning with maintenance crews throughout their respective districts in the state; and,
(4) all other Conn DOT staff who provided support for field work.

Sincere thanks appreciation are also due to members of the Connecticut Cooperative Transportation Research Program (CCTRP)/ Joint Highway Research Council (JHRAC) for their support and advice.

Additionally, the research team acknowledges the generous support provided by the Connecticut Transportation Institute (CTI) to providing lab space and administrative help throughout this project. A special thanks to members of CTI administration, including James Mahoney (Executive Director), Stephanie Merrall, John DaDalt, Scott Zenke, Anthony Lorenzetti, Carolyn Ward, and Lori Judd. Thanks to other graduate students, Suvash Dhakal, Surendra Baniya, Rishav Aryal, and Bryant Heimbach, who assisted in field installation of the bridge joint sealants.

The research team also gratefully acknowledges the material and in-kind support from BASF/Watson Bowman Acme Corp., Amherst, NY, who supplied generous quantities of its Wabo commercial silicone sealant, and also United Steel Corp., Hartford, CT, who provided steel to the research team to assemble the prototype joint.

Finally, sincere thanks and appreciation are due to the University of Connecticut and the Civil and Environmental Engineering Department for supporting and encouraging this work.

SI* (MODERN METRIC) CONVERSION FACTORS

APPROXIMATE CONVERSIONS TO SI UNITS

SYMBOL	WHEN YOU KNOW	MULTIPLY BY	TO FIND	SYMBOL
		LENGTH		
in	inches	25.4	millimeters	mm
ft	feet	0.305	meters	m
yd	yards	0.914	meters	m
mi	miles	1.61	kilometers	km
		AREA		
in^2	square inches	645.2	square millimeters	mm^2
ft^2	square feet	0.093	square meters	m^2
yd^2	square yard	0.836	square meters	m^2
ac	acres	0.405	hectares	ha
mi^2	square miles	2.59	square kilometers	km^2
		VOLUME		
fl oz	fluid ounces	29.57	milliliters	mL
gal	gallons	3.785	liters	L
ft^3	cubic feet	0.028	cubic meters	m^3
yd^3	cubic yards	0.765	cubic meters	m^3
		NOTE: volumes greater than 1000 L shall be shown in m^3		
		MASS		
oz	ounces	28.35	grams	g
lb	pounds	0.454	kilograms	kg
T	short tons (2000 lb)	0.907	megagrams (or "metric ton")	Mg (or "t")
		TEMPERATURE (exact degrees)		
°F	Fahrenheit	5 (F-32)/9 or (F-32)/1.8	Celsius	°C
		ILLUMINATION		
fc	foot-candles	10.76	lux	lx
fl	foot-Lamberts	3.426	$candela/m^2$	cd/m^2
		FORCE and PRESSURE or STRESS		
lbf	poundforce	4.45	newtons	N
lbf/in^2	poundforce per square inch	6.89	kilopascals	kPa

APPROXIMATE CONVERSIONS FROM SI UNITS

SYMBOL	WHEN YOU KNOW	MULTIPLY BY	TO FIND	SYMBOL
		LENGTH		
mm	millimeters	0.039	inches	in
m	meters	3.28	feet	ft
m	meters	1.09	yards	yd
km	kilometers	0.621	miles	mi
		AREA		
mm^2	square millimeters	0.0016	square inches	in^2
m^2	square meters	10.764	square feet	ft^2
m^2	square meters	1.195	square yards	yd^2
ha	hectares	2.47	acres	ac
km^2	square kilometers	0.386	square miles	mi^2
		VOLUME		
mL	milliliters	0.034	fluid ounces	fl oz
L	liters	0.264	gallons	gal
m^3	cubic meters	35.314	cubic feet	ft^3
m^3	cubic meters	1.307	cubic yards	yd^3
		MASS		
g	grams	0.035	ounces	oz
kg	kilograms	2.202	pounds	lb
Mg (or "t")	megagrams (or "metric ton")	1.103	short tons (2000 lb)	T
		TEMPERATURE (exact degrees)		
°C	Celsius	1.8C+32	Fahrenheit	°F
		ILLUMINATION		
lx	lux	0.0929	foot-candles	fc
cd/m^2	$candela/m^2$	0.2919	foot-Lamberts	fl
		FORCE and PRESSURE or STRESS		
N	newtons	0.225	poundforce	lbf
kPa	kilopascals	0.145	poundforce per square inch	lbf/in^2

*SI is the symbol for the International System of Units. Appropriate rounding should be made to comply with Section 4 of ASTM E380.
(Revised March 2003)

TABLE OF CONTENTS

LIST OF FIGURES

LIST OF TABLES

EXECUTIVE SUMMARY

Expansion joints are one of the most critical components of a bridge structure, as they allow for the bridge to expand and contract due to inherent temperature fluctuations. However, it has been widely known that water and deicing chemicals leakage through the joints is a major cause for corrosion and damage of the bridge structure underneath the deck. In general, one in nine bridges of the United States is rated as structurally deficient, according to the 2013 Infrastructure Report Card of the American Society of Civil Engineers. Without any doubt, leaky joints can be attributed to have played a major role in this. The poured silicone sealant joint is a very common type of bridge joint sealant because of its advantages, including: a) good durability; b) self-leveling action; c) strong elastic performance for a wide range of temperatures and UV exposures; d) ease of installation and maintenance; e) minimal cost; f) rapid curing; and, g) little to no structural impact to the bridge. Although several advantages are present, poured silicone sealant joints must be replaced every 2-3 years in Connecticut due to delamination of the sealant from the substrate.

A novel silicone foam sealant has been previously developed by the University of Connecticut (UConn) research team to remedy the current problems commonly experienced by silicone joints. This new sealant is comprised of a commercially available sealant which is chemically altered to produce more favorable mechanical properties. The chemical additives used in the sealant produce a softer, foam-like sealant. Additionally, it has been observed that the silicone foam sealant expands upon placement, which could lead to significant material savings. The main idea behind chemically modifying the sealant is to reduce its modulus of elasticity, thus reducing the stresses generated at the interface of the sealant and the substrate header.

To further evaluate the behavior and performance of the silicone foam sealant and compare them with a commercially available silicone sealant (termed here under as the solid sealant) under additional real-life practical conditions, this research project performed laboratory testing, field installation, and in-service monitoring of the foam sealant, with and without primer. For field installation, bridges were selected to include a wider gap joint and higher traffic volume than those used in the previous studies. First, tension/adhesion testing was conducted on the foam sealant using the commercially available sealant as a baseline. The failure mode and stress vs. strain of each sample was recorded, showing that the foam sealant mostly failed via cohesive rupture (i.e., rupture of the sealant itself) and maintained its bond to the header. The solid sealant, on the other hand, primarily failed via adhesive debonding from the header substrate. Next, an extensive accelerated aging study was conducted to determine and how the failure mode and stress vs. strain response is affected by laboratory aging. A large number of samples containing foam and solid sealant were aged under road salt water for several periods of time. This allowed for testing of samples at various aging times. It was observed that the foam sealant withstood the effect of aging better than the solid sealant, as the solid sealant demonstrated a more significant reduction in elastic modulus and ultimate failure stress and strain. An expansion test was also conducted to determine the effect of

expansion as a function of initial layer thickness. It was observed that a thicker layer of sealant usually expands more than a thin layer sealant.

Finally, both sealants were installed in a total of seven joints on three different bridges in the State of Connecticut to monitor their performance and allow for a realistic comparison of both sealants' in-service performance. The first bridge selected was Bridge No. 02570 on Route 6 in Windham, CT, with an average joint gap opening of 1.5 - 2 inches. The second bridge selected was bridge No. 06226 in Windsor, CT, with an average gap opening of 2.5 – 4 inches and heavier traffic volume. The third bridge selected was bridge No. 03830 on Route 22 in North Haven, CT, with an average joint gap opening of 0.75 – 2 inches. Several site visits were conducted during the next six months after installation of the sealant to assess their condition on each bridge joint. During the monitoring period, overall, fewer failures were observed on the foam sealant than the commercial solid sealant.

1.0 INTRODUCTION

This chapter discusses the motivation, objectives and scope for this research project. A literature review on various types of bridge expansion joints is also presented.

1.1 Background and Research Motivation

According to the American Society of Civil Engineers' 2013 Infrastructure Report Card, about 200 million trips are taken daily over structurally deficient bridges in the 102 largest metropolitan regions of the United States (ASCE 2013). Overall, one in nine of the nation's bridges are rated as structurally deficient. The rapidly deteriorating conditions of bridges can be largely attributed to leaky expansion joints. Expansion joints are important components in bridge structures, which are used to accommodate bridge movements due to temperature fluctuations, traffic loading, creep and shrinkage of concrete, and uneven settlement, without imposing significant secondary stress to the superstructure (Lee 1994; Dornsife 2000). Not only should expansion joints provide a watertight seal to protect the substructure from deicing chemicals and water, but they should also maintain this seal under the various movements that the bridge may experience.

Two failure modes are most often observed in bridge joints. One failure mode involves a compromise of the joint seal itself, allowing water and corrosive agents to flow under the deck and deteriorate the substructure (FHWA 1980). The other failure mode involves failure of the joint to accommodate the bridge deck movement, often due to thermal contraction and expansion. This failure is largely attributed to an improper design of the joint system. Expansion failure may result in upheaving of the road, damage to the abutment, and composite failure of the superstructure and the deck. When considering contraction failure, however, the entire deck can shift off the abutment, resulting in disaster.

Many hazards exist that, when in contact with the substructure, can degrade the integrity of the bridge itself. These include deicing salts and chemicals; cyclic movements due to vehicular loading; thermal contraction and expansion; vibrations of the structure; seismic hazards; and earth pressures/settlement (Hamilton 1985; Purvis 2003). In order for a bridge to accommodate induced movement and protect its substructure at the same time, a high-quality, long-lasting expansion joint must be installed to seal the joint effectively.

Poured silicone sealant expansion joints are one of the more popular sealing systems used in Connecticut bridges, as most bridges found in Connecticut comprise spans less than 120 feet. Spans, this small, correlate to joint gaps of less than 2 inches. The Connecticut Department of Transportation (CT DOT) reported that the average lifespan of a poured silicone sealant expansion joint when used in new construction is approximately seven years. However, when used for repairs or maintenance of old joints, poured silicone sealants joints last about three years (Milner and Shenton 2014). Common issues with poured silicone sealant joints stem from inadequate surface

preparation and poor installation procedures by maintenance crews. However, due to the low cost and easy installation of this type of joint, the silicone sealant remains an attractive option for state transportation agencies, especially when repairing small movement joints which can accommodate movements up to 1.5 inches.

Due to this continuous demand, a novel foam sealant formulation was developed to improve on the shortcomings of the currently used product (Malla et al. 2005a,b; 2006; 2007; 2011a-d; Shrestha et al. 2006). The sealant, termed "foam sealant" herein, is a chemically modified version of Wabo SiliconeSeal (WBA 2008a), the brand most commonly used by CT DOT, termed "solid sealant," herein. The research study discussed in this report summarizes the following four major tasks that were carried out as part of this study:

- Tension and adhesion testing was performed to gain a better understanding of the tensile and adhesive properties of the foam sealant and compare them to those of the commercially available silicone sealant, Wabo SiliconeSeal (WBA 2008a). The influence of primer was examined in order to gain a better understanding of whether it provides improved adhesion to the substrate under a laboratory setting.

- Further laboratory testing was performed to compare the tensile and adhesive properties of the foam and solid sealant under laboratory aging conditions. Specimens were fabricated and submersed in warm oxygenated water to simulate extended aging. Specimens were also exposed to deicing chemicals commonly found on Connecticut state roads in order to observe any deteriorating effects from both aging and salt. The influence of primer was also a variable in this experiment.

- A general application procedure was developed for in-service bridges and was used to install the joint sealing system onto three Connecticut bridges with various traffic volumes and joint gaps. The expansion joints were sealed in a systematic manner to allow for an in-service comparison of the performance of the commercially available sealant and newly developed foam sealant. This will determine if the foam sealant can be considered as a suitable alternative for small movement expansion joints.

- Regular monitoring and observation of the foam and solid sealant under in-service conditions was performed after installation. Monitoring will include records of the joint gap width due to thermal contraction and expansion, acquisition of joint movement data as a function of vehicular traffic during on and off peak hours, and regular record keeping environmental conditions.

1.2 Project Objectives

The main objective of this project is to further examine the adhesive properties of the foam sealant in comparison to the currently used solid sealant, develop an application procedure for in-service structures, install the foam sealant onto several small-movement

bridges throughout Connecticut, and evaluate its performance under real life conditions. In particular, the research involved the following steps:

- Pre-Field Laboratory Testing: Conduct laboratory tests with the new sealant to understand the sealant bonding behavior to various substrates treated with primers and larger joint gap.

- Field Installation Methods and Application: Develop a simplified procedure and method for mixing, field installation, and monitoring of sealant performance, apply the test sealants to two to three bridges in Connecticut, including heavily travelled and with larger (thermal) movement in the small joint category.

- Post-Installation Monitoring: Monitor the performance of the sealants installed under the actual field service and environmental factors, including traffic, moisture/rain, temperature, salt use, and joint movement/displacement of the bridges over the project period. Correlate the performance of the sealant with some of these more prominent factors.

- Report Preparation: Prepare quarterly, interim, and final technical reports with the results from the research. Present to the sponsor and the engineering community the results in written and oral form.

1.3 Literature Review

This section provides a literature review of the various types of bridge expansion joints used in modern construction and the advantages and disadvantages they deliver while accommodating for inherent deck movements.

The most basic type of joint, the butt joint (Figure 1), is typically used for movements less than 1 inch (Burke 1989). The opening is provided between two rigid deck slabs, which does not allow a smooth transition for traffic. Typical construction includes using a metal armoring (such as a steel angle embedded into the deck) which acts as the header. This protects the top edge of the deck from vehicle or plow impacts which may cause spalling or cracking. Advantages of the butt joint include simple and cost-effective construction. However, the obvious downside is that it easily allows penetration of water and deicing salts and chemicals, which can promote corrosion of the substructure. This joint is often found in areas of the country that do not see snow (and, therefore, ice). It is also preferred that these joints be installed on bridges with very small joint movement (i.e., less than 0.5 inches).

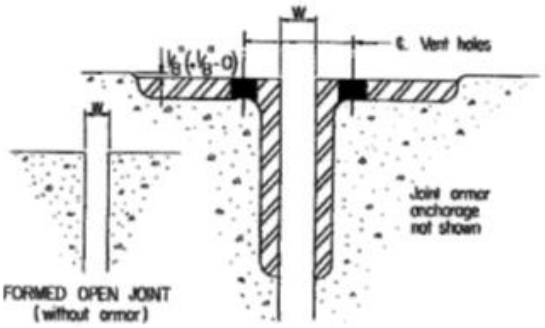

Figure 1: Typical butt joint (Burke 1989)

Sliding plate joints (Figure 2) are typically used for movements between one and three inches and bridge deck spans up to 350 feet (Lesa Systems 2016). They are simple in construction and reasonably cost-effective. The main idea behind sliding plate joints involves two overlapping steel plates being attached to the deck so that one of the plates is flush with the roadway. The plates slide against each other to accommodate various types of movements. These joints prevent debris from entering through to the substructure. Due to their reliable construction, they provide a good barrier for a long period of time. The down-side of the sliding plate joint, however, is that they do not provide an effective seal against water intrusion or deicing chemicals. Additionally, small particles of debris such as sand or glass can get stuck in between the plates and cause unwanted friction which may lead to wearing of the plates over time.

Figure 2: Typical sliding plate joint (Lesa Systems 2016)

Compression seal joints (Figure 3) comprise continuous elastomeric sections with an internal web structure that allows for expansion and collapse of the seal to accommodate deck movements between 0.25 to 2.5 inches (MM System 2015). Since this seal features an elastomeric material, it is very flexible in accounting for horizontal and vertical deck movements. Additionally, the compression seal is effective in sealing the joint from water and debris infiltration. The down side of this joint, however, is that it is highly susceptible to damage from snowplows and other sharp debris. Additionally, this seal may lose its adhesion to the substrate.

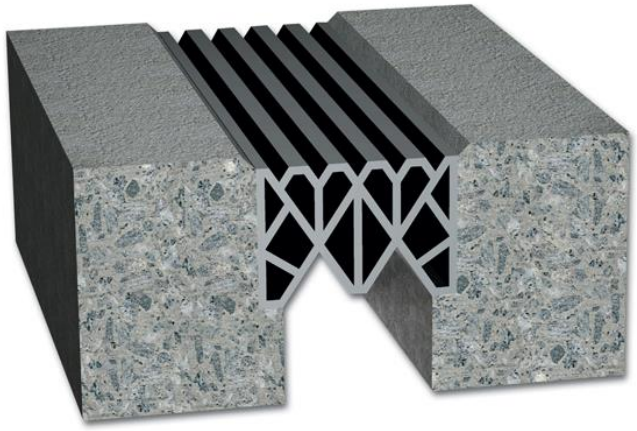

Figure 3: Typical compression seal joint (MM Systems 2015)

Perhaps the most popular joint in New England (especially in Connecticut), the asphaltic plug joint (APJ), provides a watertight seal with essentially no long term traffic disruption during installation. These joints can accommodate movement of up to 1.5 inches. As shown in Figure 4, polymer-modified asphalt (PMA), is poured in a carved channel between two bridge decks sealed by a backer rod and a bridging plate (USC 2015). Prior to pouring of the asphalt, the channel is prepared with waterproofing and a wearing surface to ensure proper adhesion to the concrete deck. A drainage tube, which deviates water away from the joint, is also installed in the event that water penetrates through the seal. Once the modified asphalt is sufficiently cured, it will accommodate traffic, thermal and impact loadings, as it has excellent contraction and expansion properties. The main downside of APJs is the softening and creeping of the material under high temperatures. This often leads to rutting and detachment of the asphalt from the substrate, resulting in an expensive cleaning and replacement process. Additionally, the polymer modified concrete can crack in cold temperatures, allowing water and chemical penetration. The relaxation of the asphaltic plug joint should be sufficient to relieve the stress due to applied thermal displacement (Bramel et al. 2000). Asphaltic plug joints are not typically installed for vertical or skewed joints.

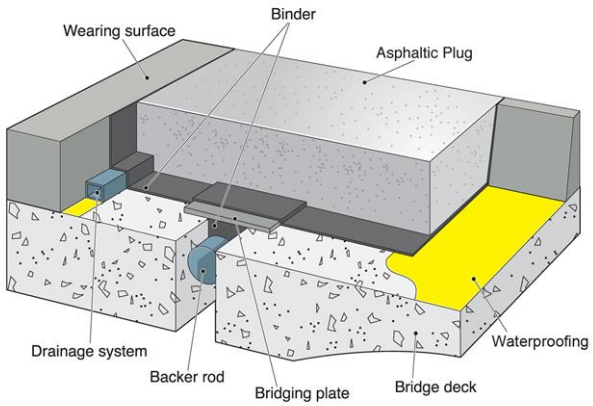

Figure 4: Typical asphaltic plug joint (USC 2015)

A typical poured silicone joint (Figure 5), which can accommodate bridge movements between 0.25 and 1.5 inches, is usually installed on shorter span bridges where the movement is minimal (BASF/WBA 2015). Such joints consist of a backer rod inserted between two bridge decks onto which the silicone sealant is poured (Dow Corning 2004a). The backer rod is typically made of compressible, temperature resistant, UV-resistant foam to accommodate various movements but still keep the silicone in place throughout the lifespan of the joint. Poured silicone sealant joints exhibit several advantages, including good durability, self-leveling action, strong elastic performance for a wide range of temperatures and UV exposures, and rapid curing, allowing for minimum traffic disruptions during installation (Fincher 1983). The most common problems with poured silicone joints include detachment of the silicone from the substrate and mechanical damage to the silicone material due to accumulation of debris and salt.

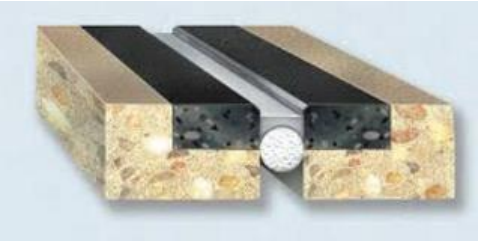

Figure 5: Typical poured silicone sealant joint (BASF/WBA 2015)

A strip seal (Figure 6) typically consists of a "V"-shape neoprene gland which is mechanically locked into a metal facing located on the header of the joint (DSB 2015). Movement is accommodated by unfolding of the elastomeric gland. This gland provides a waterproof seal which protects the substructure of the bridge from water and road salts. However, if debris gets caught inside the gland, the joint becomes vulnerable to puncture once the gland closes during the summer season when the bridge joint is narrowest. Additionally, faulty installation or dirty locking devices can cause pulling out of the gland from the metal rail edges.

Figure 6: Typical strip seal joint (DSB 2015)

Finger joints (Figure 7), which are applicable for bridge movements of 3 inches or greater, are one of the most dependable expansion joints for larger movement bridges (Tensa 2015). They allow debris and water to enter, but a diaphragm that hangs between the two bridge decks catches any unwanted material and allows it to flow out to the sides of the bridge deck. Finger joints can accommodate for rotational and vertical movement, which can be crucial for medium movement bridges (especially in seismic regions). Some problems of the finger joint, however, include damage to the "fingers," which may lead to them bending upwards. This can result in a rough bump for vehicles or puncturing of the tires. Additionally, the diaphragm that hangs below the roadway must be constantly cleaned to prevent buildup of debris. This operation may prove to be costly and time consuming.

Figure 7: Typical finger joint (Tensa 2015)

Modular bridge joints (Figure 8), designed to accommodate bridge deck movements as large as 24 inches, are the most complex and expensive expansion joints (DSB 2015). They are designed to provide a watertight seal while maintaining smooth wheel load transfer between decks. Since they can accommodate movement up to 24 inches, the joints themselves can be rather large, sometimes spanning over five feet. The system comprises a series of center beams supported atop support bars. The center beams are oriented parallel to the joint axis, while the support bars are placed parallel to the movement direction and are usually embedded into the concrete deck as a monolithic connection. Although these joints are capable of handling large thermal movements, making them great candidates for long-span bridges, concerns raised with this type of joint include fatigue cracking of welds, damage to the neoprene sealer material, damage from snowplows, and debris getting caught in between the modules. In addition, many state transportation agencies are reluctant to use modular joints because of their high initial costs and expensive and tedious maintenance patterns.

Figure 8: Typical modular bridge joint (DSB 2015)

1.4 Design of Bridge Expansion Joints

The American Association of State Highway and Transportation Officials (AASHTO) is the standards-setting body which establishes protocols and guidelines which are used in the design and construction of highways in the United States. The AASHTO (2012) version outlines procedures for the design and installation of expansion joints to accommodate movements due to temperature changes, creep and shrinkage, elastic shortening due to pre-stressing, traffic loading, construction tolerances, or other effects. The joints must be detailed to prevent damage to the structure from water, deicing chemicals, and roadway debris (AASHTO 2012). To determine the most applicable expansion joint, the anticipated movement of the bridge must be examined. Additionally, the designer must select the criteria for the joint regarding desired performance, durability, service life, maintenance requirements, joint details at the interface, initial costs, climate conditions, installation procedures, life-cycle costs, and service level (Purvis 2003).

The most basic procedural step when selecting a suitable type of expansion joint is to assess the anticipated movement of the bridge deck due to thermal contraction and expansion, as this phenomenon is inherent and must be accommodated for from the start. Thermal contraction and expansion will most likely produce the largest joint gap movement throughout the course of a year, especially in regions that experience seasonal temperature swings. CT DOT typically designs bridge joints to accommodate anticipated thermal movements due to temperature ranging from −10 to 110 °F (CT DOT 2003). This temperature range varies for each state, especially for states that experience more consistent climates than states which see all four seasons. Equation 1 shows the most common method of estimating total anticipated deck movement, $\Delta_{T,}$ between a specific temperature range, T_{max} and T_{min} based on the thermal coefficient, α, of the material and span length, $L_{deck,}$ of the bridge.

$$\Delta_T = \alpha L_{deck}. (T_{max} - T_{min}) \quad (1)$$

Table 1: Coefficient of thermal expansion for various materials

Material	Coefficient of Thermal Expansion, α (μm/m/K)
Aluminum	22.2
Concrete	12
Iron	10.4
Rubber	77
Silicone	3
Steel	11

Table 1 shows that the coefficients of thermal expansions for steel and concrete are 11 and 12 K^{-1}, respectively. These materials, the primary ones used in bridge construction throughout Connecticut (CT DOT 2001), have a similar coefficient of thermal expansion, which results in a uniform movement of the composite section.

1.5 Structure of Report

Section 1 introduces the importance of expansion joints and bridges and outlines the various types of joints that can accommodate for a range of movements. This section also outlines the motivation behind the research and the project objectives. Section 2 presents the laboratory tests that were conducted to gain a better understanding of the silicone sealants' properties under tensile loadings. The tests were designed in such a way to evaluate the performance of both sealants, with and without the presence of primer and road salt under controlled curing and accelerated aging. Several experiments are also outlined in this chapter; these experiments provided scientific information about the foam sealant. Section 3 describes the field installation phase of the project, where both sealants (foam and solid) were installed on three in-service bridges throughout the state of Connecticut. The installation procedure was designed to allow for comparison of the performance of both sealants in a real-life scenario. Consequently, Section 4 shows the field-monitoring phase of the project which sheds light on the demands on the sealing system. A traffic counter was installed on one bridge to determine the vehicular demand on the joint, and displacement measuring devices were installed on two of the bridges to assess the movement of the structure itself. Section 5 presents summary, conclusions and recommendations for future work. Finally, Section 6 presents a list of publications cited in this document.

2.0 LABORATORY TESTING

2.1 Background

Previous experiments conducted by Malla et al. (2005a,b; 2006; 2007; 2011a-d) included extensive laboratory testing of the foam sealant using the same formulation to better understand the mechanical behavior of the sealant. Mechanical properties, such as shear strength and tensile strength, have been assessed, and compared to the commercially-available solid sealant. Once basic properties were established, a closer examination of the results showed that the foam sealant typically failed cohesively (i.e., ripping of the silicone material) as opposed to the solid sealant, which failed adhesively (i.e., detachment from the substrate). Results also showed that the foam sealant exhibited a lower modulus of elasticity while maintaining a comparable ultimate strain capacity. Because of the lower modulus of elasticity, the ultimate stress capacity was also lower than that of the solid sealant. Although a lower capacity may not be favorable in civil engineering materials, the ultimate capacity was achieved at an elongation of approximately 900%, which is much larger than what an average bridge gap will expand.

2.2 Experimental Motivation

Several state transportation agencies (Illinois and Connecticut, among others) encourage the application of primer onto the substrate prior to installation of the silicone sealant, as it promotes a cleaner, oil-free surface onto which the sealant will bond (IL DOT 2011; Tremco 2014). However, some manufacturers claim that no primer is needed with their products (WBA 2001; 2008c). Little research has been conducted on the effectiveness of primer on the adhesion of silicone sealant joint systems, especially in bridge structure applications. Therefore, the inclusion of primer in laboratory experiments is of high interest.

In addition to the inclusion of primer, a primary concern for the degradation of silicone sealant joint systems is the effect of deicing chemicals, which are prevalent in Connecticut during the winter months. It has been well established that road salt corrodes and deteriorates concrete and steel. Due to silicone's excellent chemical resistance, however, a key aspect of laboratory testing is to determine whether the bond between the silicone and concrete (typical header material) degrades under the presence of deicing chemicals such as sodium chloride and magnesium chloride, the two most common chemicals found on state roads during the winter (CT DOT 2015).

The motivation behind conducting laboratory testing was to observe the behavior of the foam sealant in contrast to the solid sealant with and without the presence of primer. Currently, specifications regard primer as being optional but encouraged; the true effect of the primer, however, is unknown. Therefore, the tension and adhesion test included specimens containing primer to determine how the sealant bonds to the substrate when primer is applied. Additionally, the aging experiment contained specimens with primer as well. A density test was conducted in order to determine the density of the foam sealant,

as it is suspected that the foam sealant exhibits a lower density compared to the solid sealant because of the expansion effect. An expansion test was also conducted in order to quantify how much the foam sealant expands as a function of initial volume. Finally, a prototype joint was fabricated to test larger scale mixing and application to prepare for field installation. The results of all experiments are presented in the following section.

2.3 Overview of Foam Sealant Formulation

A poured silicone sealant expansion joint system previously developed by Malla, et al., (2005a,b; 2006; 2007; 2011a-d) is considered as a suitable, cost-effective joint sealing system that allows for a long term sealing solution for smaller movement bridges. The sealant, termed "foam sealant" herein, comprises of Wabo SiliconeSeal (WBA 2008a), (a commercial brand commonly used by CT DOT), water, crosslinker (Momentive Materials) and a platinum catalyst (Gelest 2003).

Without any additives, Wabo SiliconeSeal (termed "solid sealant" herein) produces a solid, rubber-like material; with the addition of the remaining ingredients, foaming of the silicone occurs due to the reaction of water with the added hydrosilane, producing silanol groups and hydrogen gas. As the foam sealant cures over time, the hydrogen gas produces bubbles within the silicone, while the silanol groups condense and expedite the polymerization (and, thus, curing) of the material. A schematic of the chemical reaction is shown in Figure 9.

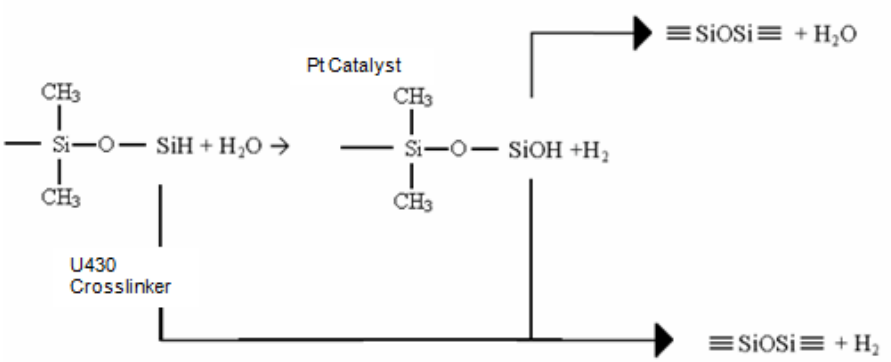

Figure 9: Schematic of foam sealant reaction (Malla et al. 2007)

The modified formulation produces a foam-like silicone sealant, which has been observed to expand approximately 70% of its initial volume (Malla et al. 2005, 2006; 2007; Swanson et al. 2013). Previous studies have shown that the foam sealant exhibits a significantly lower modulus when compared to the commercial (solid) product. This characteristic is especially important, as it decreases the stresses at the interaction surface between the bridge header and the sealant, itself, and, thus, reduces the likelihood of premature adhesive failure.

2.4 Mixing Protocol for Experiments

A consistent mixing process was established in order to maintain consistency for all experiments (ASTM 2009). As with many materials that require mixing, such as concrete, the quality of the sealant often depends on the skill and experience of the user. Therefore, several trial mixes were conducted prior to the actual experiments to establish a feel for the material and produce the same consistency of material for each subsequent mix. Before beginning the mixing process, all components listed in Table 2 were weighed out by mass and placed aside to minimize wasted time between adding ingredients (Figure 10). A mixing paddle was used to stir all ingredients together as outlined by the Watson Bowman specifications for mixing their commercial sealant. First, Wabo White (part A) and Wabo Grey (part B) were combined and mixed until a thorough consistency was achieved. Next, platinum catalyst was slowly added, followed by water. These components were added while continuously stirring the sealant. Once the added components were mixed in with the sealant, the crosslinker was added to initiate the chemical reaction. Mixing continued until the entire mixture exhibited a uniform texture.

Table 2: Mix proportions for foam sealant

Component	Density (g/cm^3)	Percent Volume (%)
Wabo White (A)	1.08	54.43
Wabo Grey (B)	1.45	40.54
Crosslinker	0.98	2.77
Water	1	1.8
Platinum Catalyst	0.98	0.46

Figure 10: (Left to right) Wabo, crosslinker, water, platinum

A consistent mixing procedure is important, especially because a small deviation in quantities added or mixing technique can alter the properties of the foam sealant. Care was also taken to mix enough material to ensure the same batch of material was used for

each experiment without mixing more material for the same set of specimens. The mixing procedure is illustrated in Figure 11.

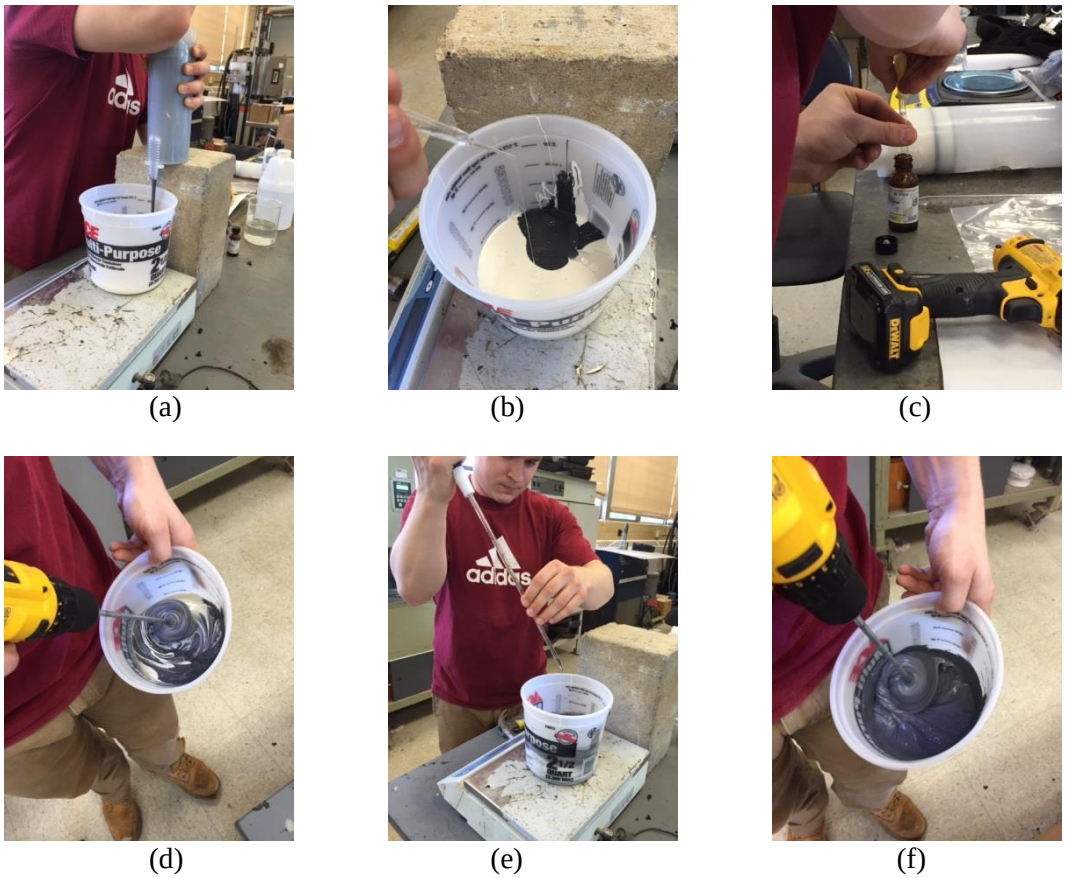

(a) Pouring equal parts by volume of Wabo black and grey
(b) Addition of water through dropper
(c) Addition of platinum catalyst through dropper
(d) Mixing of first four ingredients for about 45 seconds (time varies with initial volume)
(e) Addition of crosslinker with pipette
(f) Mixing of all five ingredients for about 45 seconds (time varies with initial volume)

Figure 11: Mixing procedure for foam sealant

2.5 Fabrication of Test Coupons

All laboratory tests involving evaluation of mechanical properties consisted of creating specimens containing either solid or foam sealant. These specimens were used for the tension/adhesion experiment and also for the aging experiment. Specimens were cast and fabricated similarly to those used in previous studies by Malla, et al., (2005; 2006; 2007) as shown in Figure 12.

The tension/adhesion experiment's test coupons were made of concrete and steel, the two most common substrates found in newly constructed bridges. First, the appropriate

materials were obtained to adequately replicate those present in the field. With the assistance of CT DOT, a large piece of concrete was salvaged from a local bridge undergoing replacement. This was done to reflect the type of concrete in joint headers, typically found throughout the state. Steel was also obtained with the assistance from UConn's Civil Engineering machine shop. Blocks were fabricated using typical A36 steel, the material commonly found at the joints of bridge decks with angle headers. Each specimen contained a 12.7 x 50.8 x 12.7 mm (0.5 x 2 x 0.5 in.) volume of sealant applied in between two substrate blocks measuring 76 x 50.8 x 12.7 mm (3 x 2 x 0.5 in.) (LxWxH).

Figure 12: Fabrication of coupons for experimental testing

The substrate chosen for specimens in the aging experiment was a polymer modified concrete (WaboCrete II), selected specifically because of its common use in bridge header repair throughout the state of Connecticut. This concrete mix, manufactured by Watson Bowman Acme Corporation (WBA 2008b), is composed of three components: the activator (part A), the resin (part B), and the aggregate. The aggregate contains a particle size distribution between 0.08 and 15 mm, having 30-65% passing through a 2-mm screen, 12-15% passing through a 0.08-mm screen, and 100% passing through a 15-mm screen. Per manufacturer specifications, the resin was premixed separately for about 20 seconds before being mixed with the activator in a 5-gallon bucket for approximately 30 seconds. The aggregate was then added until every particle was coated in the mixture. Once all specimens were cast, they were left to cure at room temperature (23 ± 2^0C) for 14 days as shown in Figure 13. Upon full curing, the blocks were cut into coupons to create test specimens, as shown in Figure 14.

Figure 13: Formwork for polymer modified concrete casting

Care was taken to cast the specimens with exact dimensions (including sealant dimensions). Due to the expansion effect of the foam sealant, and inherent imperfections, some specimens contained sealant with slightly varying heights; therefore, exact dimensions of each specimen were recorded using a caliper for any anticipated adjustments in future calculations of mechanical properties.

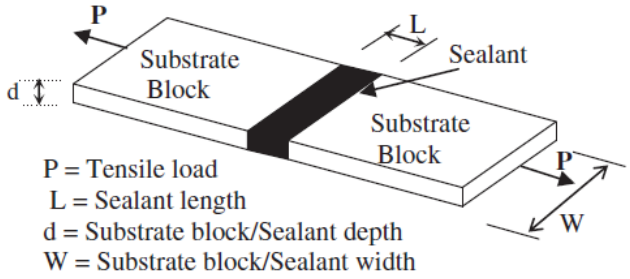

Figure 14: Typical test specimen (Malla et al. 2007)

2.6 Application of Primer

Some specimens contained substrate blocks treated with primer in order to compare the adhesion characteristics of each sealant under the influence of primer. The primer, manufactured by Dow Corning (2004b,c) , was selected in accordance to the appropriate substrate. Dow Corning 1200 OS Primer was used for specimens containing a concrete substrate. Dow Corning Primer P was used for specimens containing a steel substrate (Figure 15). Per Dow Corning specifications, the substrate was first cleaned with a lint-free cloth to remove any dust or residue. A light coating of primer was applied using a brush. After approximately 90 minutes of drying, the sealant was cast into the gap between the substrate blocks.

Figure 15: Primer for steel (left) and concrete (right)

2.7 Tension/Adhesion Test and Results

The tension and adhesion test was designed to observe the effect of primer application on each type of sealant (foam and solid) while evaluating the tensile and adhesive properties of each sealant. Five (5) specimens were fabricated for each variable tested: foam sealant with primer, foam sealant with no primer, solid sealant with primer, and solid sealant with no primer. Since two substrates (concrete and steel) were considered, a total of forty (40) specimens, similar to the ones shown in Figure 16, were fabricated for this test. Twenty (20) specimens contained sealant applied in between two concrete blocks, and the other twenty specimens contained sealant applied in between two steel blocks with the same dimensions.

Figure 16: Concrete and steel coupons prepared for pouring of sealant

Upon casting, all forty specimens cured at room temperature (23 ± 2^{0}C) for 14 days. Upon completion of curing, each specimen was labeled and installed at random onto an Intron Model 1011 tensile tester and pulled until failure. Loads were measured using a 500-N (100-lb.) load cell. The testing procedure was modeled on specifications outlined by ASTM C1135-00, Standard Test Method for Determining Tensile Adhesion Properties of Structural Sealants (ASTM 2000). As shown in Figure 17, both substrate blocks were gripped using the mechanical clamps attached to the machine. The lower end of the specimen's concrete block was fixed while the other concrete block was extended at a rate of 10 mm/min. Using displacement control, the machine recorded the tensile force required to extend the specimen over a specific displacement. From this data, stress and strain information was extracted and computed.

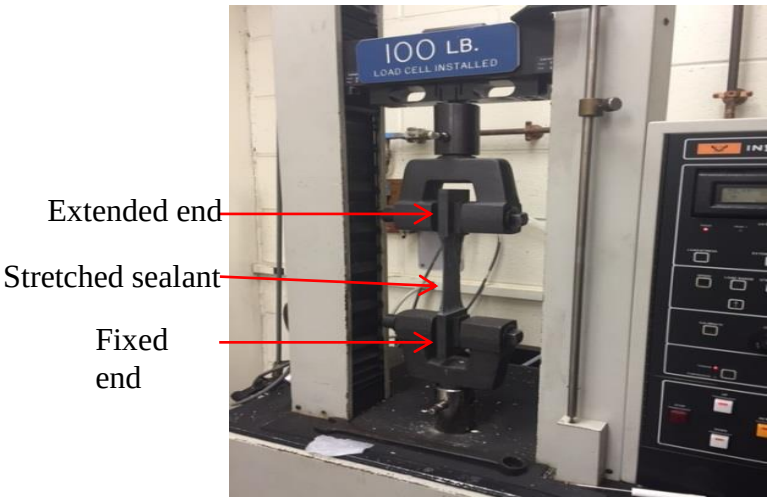

Figure 17: Tensile testing using Instron machine

After testing five specimens per variable for each substrate (concrete and steel), both results revealed the foam sealant has a lower tensile modulus (compare Figures 18 and 19). In addition, Figures 18 and 19 show that ultimate stresses and strains for specimens containing foam sealant were lower than those containing solid sealant. Specifically, specimens containing foam sealant exhibited an average ultimate stress of 155 kPa while maintaining an average ultimate strain of 922.5%. Meanwhile, the solid sealant exhibited an average ultimate stress of 312 kPa with a corresponding average ultimate strain of 1027%. While the foam sealant showed a smaller average strain, the corresponding ultimate stress is about 49% of the solid sealant's ultimate stress capacity. Although typical civil engineering materials are characterized by their ultimate capacity, this reduction in ultimate stress is actually favorable for reducing the stresses at the interface of the silicone sealant and the bridge header. There was no significant difference observed in maximum stress or strain properties of the specimens between steel and concrete substrates.

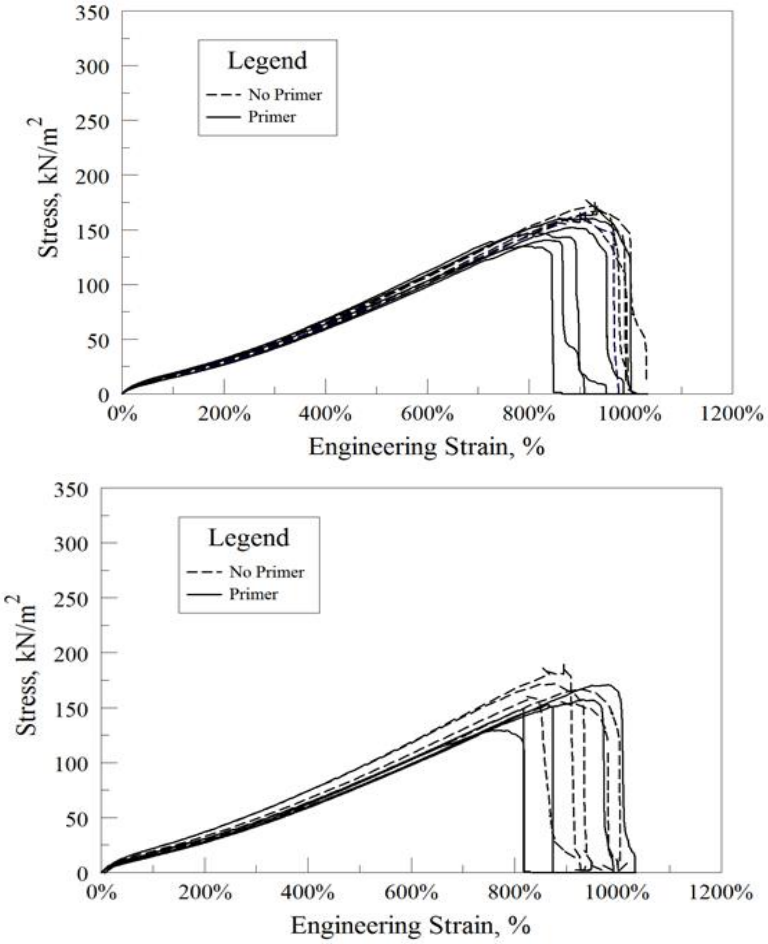

Figure 18: Results for specimens containing foam sealant, steel substrate (top) and foam sealant, concrete substrate (bottom)

The key characteristic that can be taken from this experiment is the failure mode of each specimen. Figures 18 and 19 show the stress vs. strain curves of each specimen; although the strain ranges are comparable, and an obvious reduction in modulus is observed in the specimens containing foam sealant, all solid sealant specimens exhibited an adhesive failure, while the foam sealant specimens failed via cohesive failure. Adhesive failure is characterized by detachment of the sealant from the substrate prior to material failure. Cohesive failure, on the other hand, pertains to ripping or shearing of the silicone material itself while maintaining its attachment to the substrate. Both failure modes can be observed in Figures 18 and 19, as a cohesive failure is characterized by a smooth, rolling peak as the stress approaches its ultimate limit state. Adhesive detachment, however, can be seen when the stress peak sharply drops, indicating a sudden failure under tension. Cohesive failure was observed in 100% of the specimens containing foam sealant for both substrates (concrete and steel). For specimens containing solid sealant, however, 90% of the specimens failed via adhesive failure. Figures 20-23 show the specimens post failure.

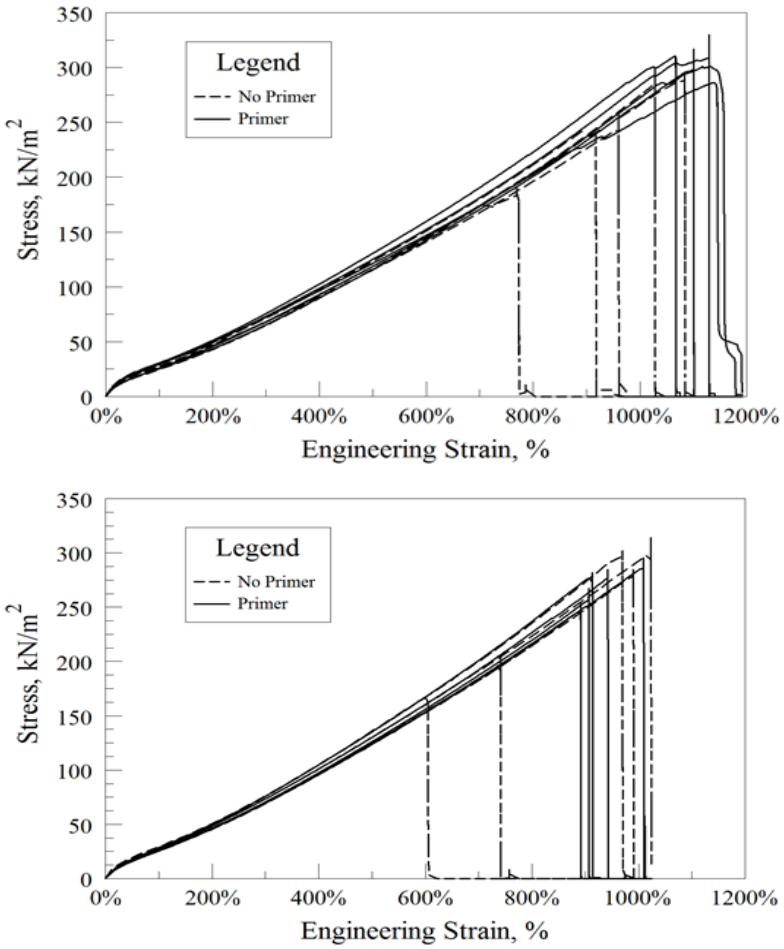

Figure 19: Results for specimens containing solid sealant, steel substrate (top) and solid sealant, concrete substrate (bottom)

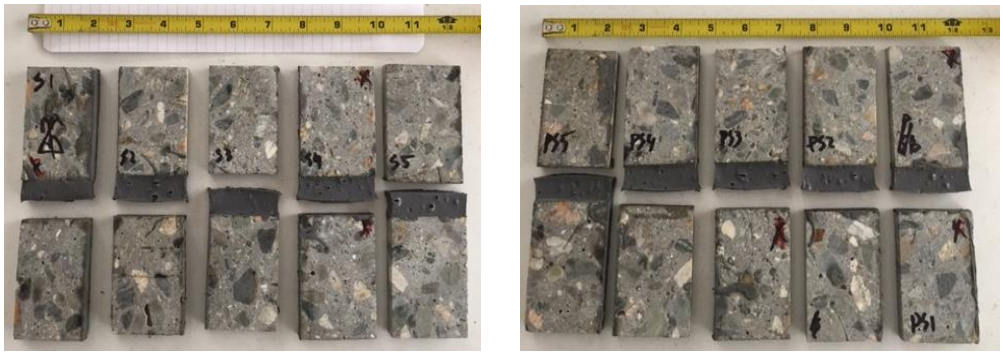

(a) **(b)**

Figure 20: Concrete specimens containing (a) solid sealant with no primer; (b) solid sealant with primer

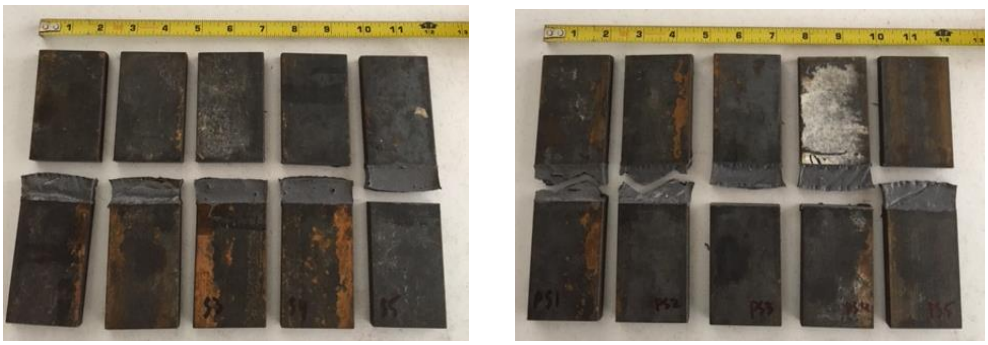

(a) **(b)**

Figure 21: Steel specimens containing (a) solid sealant with no primer; (b) solid sealant with primer

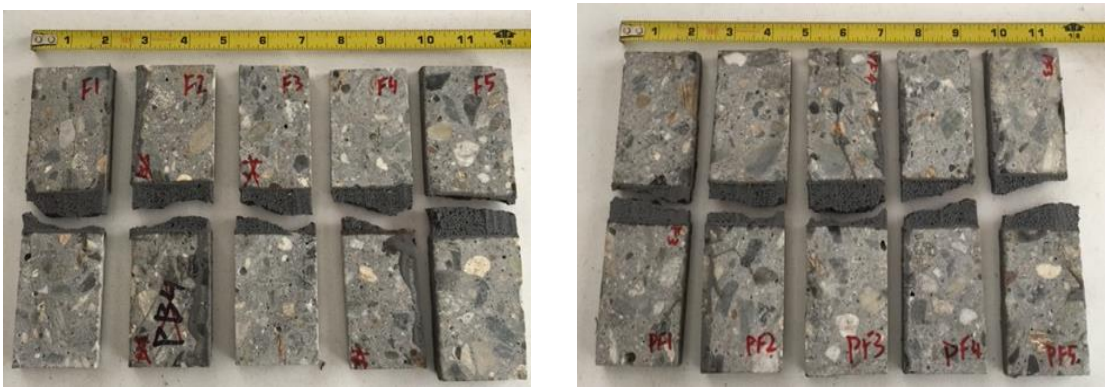

(a) **(b)**

Figure 22: Concrete specimens containing (a) foam sealant with no primer; (b) foam sealant with primer

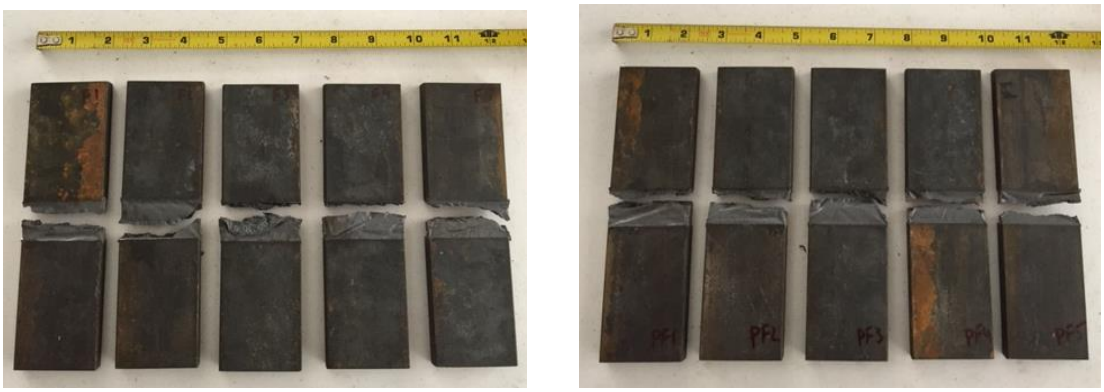

(a) **(b)**

Figure 23: Steel specimens containing (a) foam sealant with no primer; (b) foam sealant with primer

The failure modes for specimens treated with primer were very similar for those that were not treated. When primer was applied to solid specimens, 20% of them failed via cohesive failure, while 80% still failed by means of detachment from the substrate. Although primer was applied, the conclusion that primer improves bonding of the sealant to the substrate cannot be made from these results. Specimens containing foam sealant

and primer still exhibited excellent bond as all specimens failed cohesively, as expected. The breakdown of average ultimate stress, average ultimate strain, average modulus at 100% strain, and failure mode fraction is shown in Table 3. Figures 24-25 show a graphical comparison of average ultimate stress for each substrate.

Table 3: Results for tension/adhesion test

Substrate	Sealant Type	Primer Presence	Average Ultimate Stress (kPa)	Average Ultimate Strain (%)	Average Modulus at 100% Strain (kPa)	Failure Mode	
						Cohesive	Adhesive
Concrete	Foam	Yes	161	906	16.06	5	0
	Foam	No	158	952	19.62	5	0
	Solid	Yes	318	933	24.1	0	5
	Solid	No	246	866	26.6	0	5
Steel	Foam	Yes	149	939	16.81	2	3
	Foam	No	164	998	17.01	0	5
	Solid	Yes	306	1121	28.38	5	0
	Solid	No	265	953	28.03	5	0

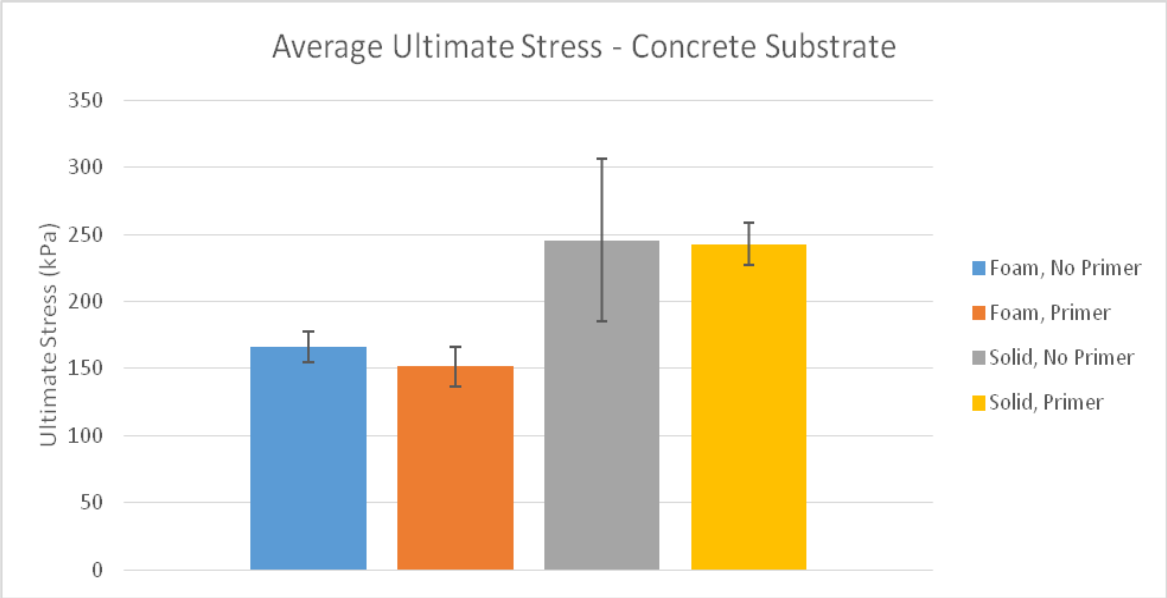

Figure 24: Average ultimate stress for specimens with a concrete substrate

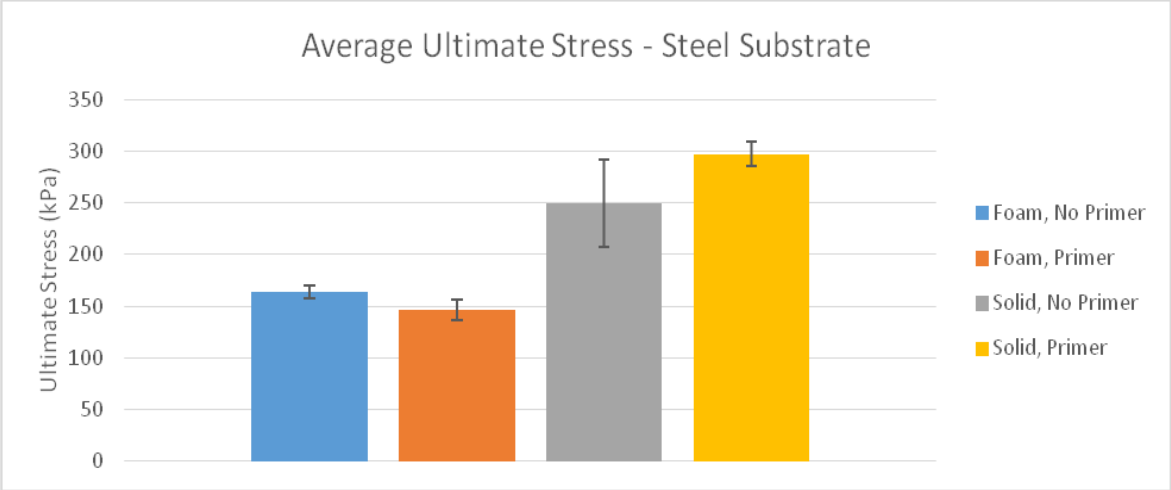

Figure 25: Average ultimate stress for specimens with a steel substrate

2.8 Aging/Salt Water Test and Results

Similar specimens were used for the aging/salt corrosion test as the ones used in the tension and adhesion experiment. Motivation to conduct this aging study stemmed from the potential degradation of the bond between the sealant and substrate over time, especially in the presence of moisture. Real time aging was simulated by utilizing hot water aging methods as specified in ASTM C1560-03 (ASTM 2003). It was envisioned that specimens would be removed from the aging environment at various time intervals and tested for adhesion and tensile strength by pulling them to failure at each respective aging period. Seven testing periods, or durations of accelerated aging, were established: 0 days, 14 days, 1 month, 2 months, 3 months, 4 months and 5 months.

Five (5) specimens per variable (foam sealant with primer; foam sealant without primer; solid sealant with primer; solid sealant without primer) were cast for each testing period. Therefore, one hundred and forty (140) samples were fabricated to be tested at each time interval, including zero days aging. Since the effect of road salt exposure on aged specimens is also of interest, another set of 140 specimens were cast, yielding a total of two hundred and eighty (280) specimens in total (Figure 26).

Figure 26: Curing of sealant specimens with concrete substrate for aging experiment

Each tank was heated to 95 °F (35 °C) using a 400-W submersible water heater with a sensor and activator. The temperature for both tanks was kept to a strict deviation tolerance of ± 1 °F(± 0.55 °C). Temperature profiles of each tank were recorded regularly (Figure 27). The low temperature in each tank observed on day 10 was due to a power outage of the building in which the tanks were located; however, power was restored within 6 hours and the target temperature was regained shortly afterwards.

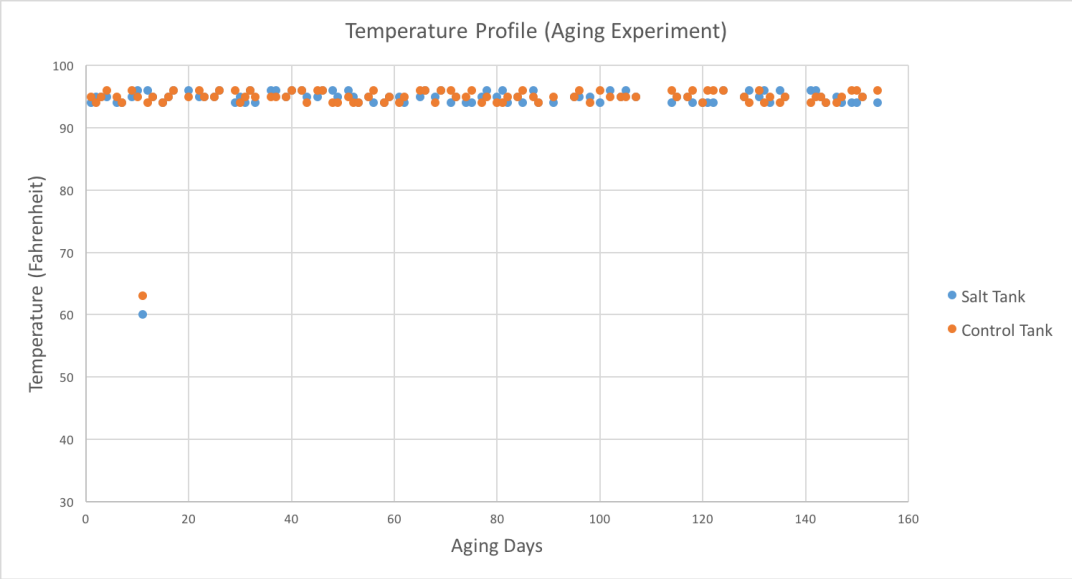

Figure 27: Temperature profile of water tanks

One tank contained water with no additives and the other tank contained a saturated solution of water mixed with sodium chloride and magnesium chloride. This experimental design enabled for observation of the effects of aging and also the effects of

aging with the influence of road salt. Concentrations of sodium chloride and magnesium chloride per total solution volume were 38.72% and 2.03%, respectively. These proportions are specified by CT DOT as mandatory minimum dispensing ratios for chemical treatment of state roads (CT DOT 2015). After thorough mixing, the pH of the solution was measured to be 8.52.

To simulate adequate aging, oxygen was delivered to the specimens through two air pumps located at the bottom of each tank. The purpose of these pumps was twofold; they supplied oxygen to the specimens and also provided circulation to the water to ensure an even temperature distribution and prevent salt particles from settling to the bottom of the test tanks. The specimens were arranged on five open-area racks per tank, allowing for maximum exposure to the water. Since the water heaters were placed at the bottom of the tanks, the specimens closer to the heater may experience a warmer aging environment. To reduce the proximity bias, the racks were rotated systematically, twice per week, to ensure all specimens experience the same aging environment. Throughout the course of the experiment, the tanks were covered on all sides with insulation to reduce heat loss. The experimental set up is shown in Figure 28.

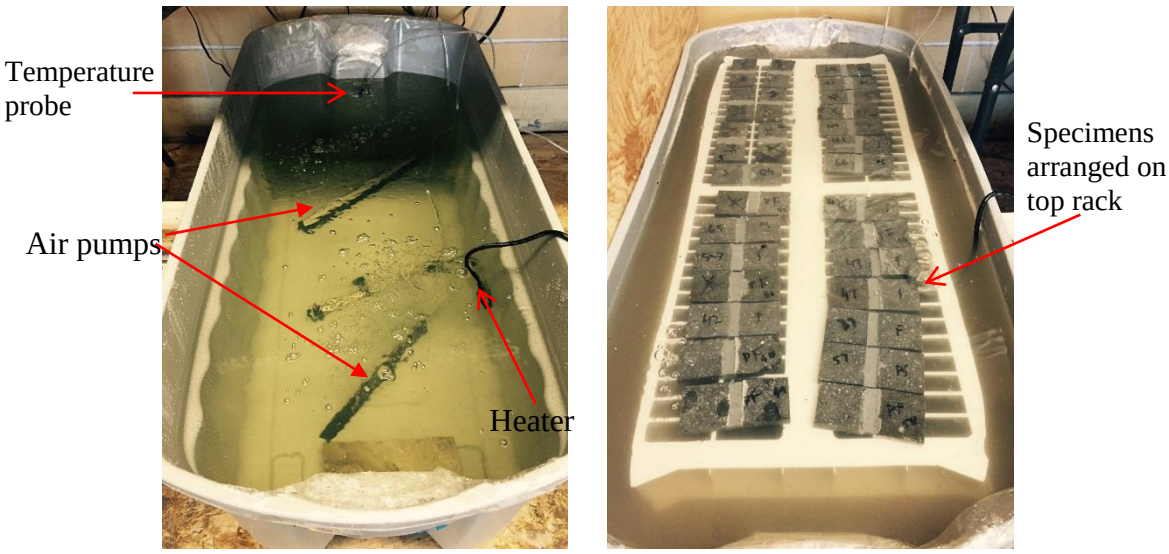

Figure 28: (a) Placement of heater and air pumps, (b) water tank containing 140 specimens

Due to the large number of specimens, the testing protocol was designed to minimize any changes in procedure throughout the course of five months. Therefore, upon each aging period, the specimens were removed from the tanks and rinsed with warm water to remove any salt or residue that may have accumulated over time. The specimens were then stored in a refrigerator at 42^{o}F to ensure a cold, dark and consistent environment. This significantly slowed down any additional aging, especially for the specimens extracted at early aging durations. After the completion of five months, all specimens were extracted from the refrigerator and tested at the same time. However, due to the large number of specimens (280), the last specimen was tested six days after the first.

Upon extraction from the refrigerator, the specimens were labeled according to a random number generator. These numbers represented the order in which they would be tested (this minimized the bias in testing certain types of specimens before others). Since there were a large number of specimens, this also ensured that the testing procedure was not different for a specific bundle of specimens than for others.

The testing procedure was based on ASTM C1135 Standard Test Method for Determining Tensile Adhesion Properties of Structural Sealants (ASTM 2000). However, the procedure deviated slightly from the specified standard because a lower rate of extension was implemented (10 mm/min instead of 50 mm/min). Similar to the tension/adhesion test, the specimens were installed onto the Instron model 1011 (Instron 2010) and, using a 1000-pound load cell, pulled to failure. Because of the shape and dimensions of the substrate blocks (the dimensions of the substrate blocks exactly matched the dimensions of the grips of the Instron machine), the specimens were mounted in the same way for each test. This was important, as a slight angle in mounting would have an important effect on the measured values.

Inherent imperfections existed within each specimen due to slightly varying thicknesses of sealant. This was also because of the expansion of the sealant, which varies depending on the thickness of the initial layer. To account for this in future calculations, the thickness of each specimen was measured using a digital caliper and recorded for future adjustments. Per ASTM standards for tensile testing of structural sealants (ASTM 2000), the mode of failure, ultimate extension, and ultimate force were recorded upon failure. From these results, stress and strain properties were calculated and tabulated (Kruszewski 2016). The test setup is shown in Figure 29.

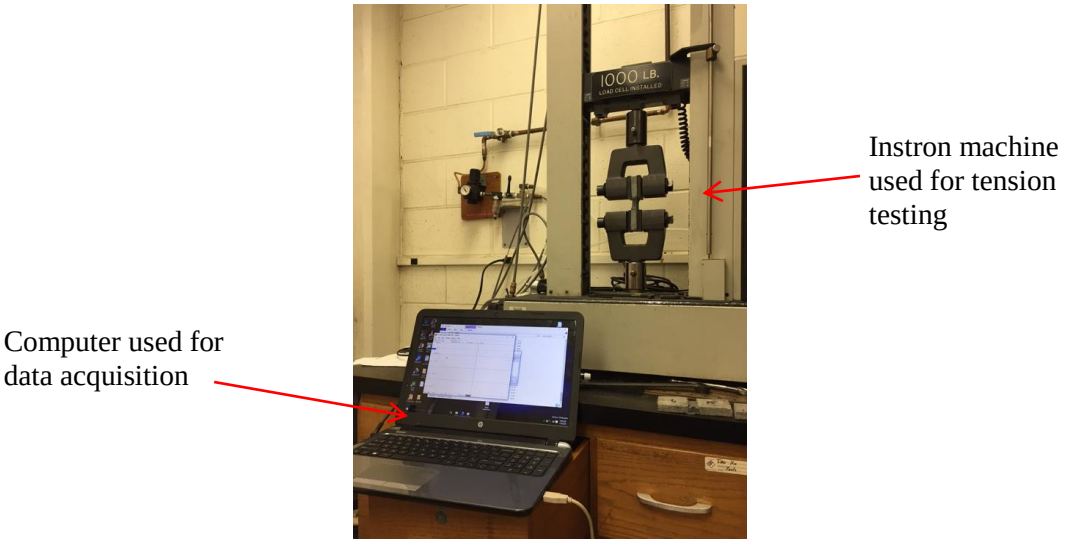

Figure 29: Experimental setup containing Instron machine and data acquisition system

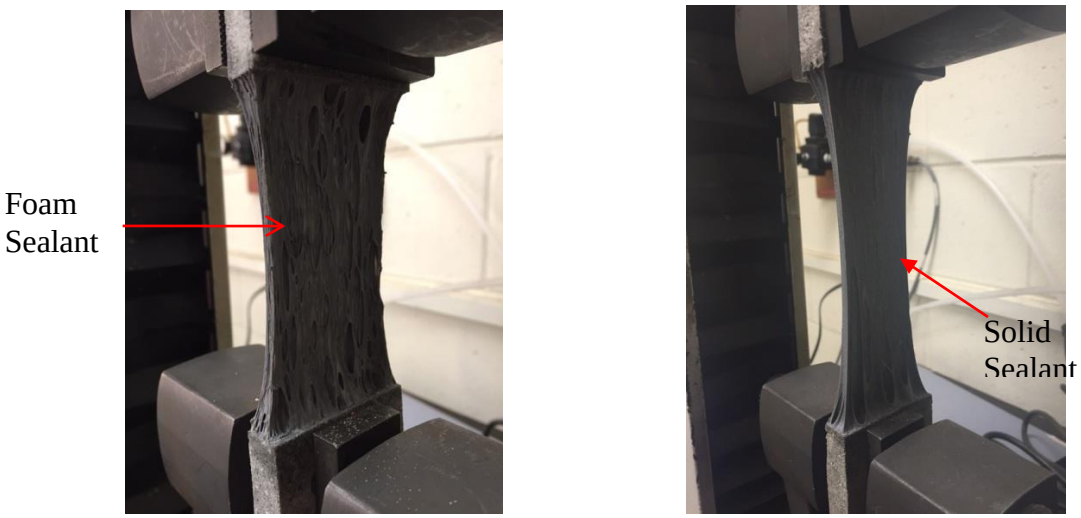

(a) (b)

Figure 30: Condition of extended specimens containing (a) foam sealant and (b) solid sealant

Figure 30 shows the extent of the air pockets formed for specimens containing foam (compared to the containing solid sealant). A common observation among foam specimens was that the cohesive mode of failure initiated at regions where large air pockets were stretched. Upon further stretching, these air pockets began to tear longitudinally, creating weak points in the structure of the sealant. Upon even further extension, the sealant grew thin and eventually yielded, creating a hole in the sealant. Once this hole developed, the remaining sections of the sealant were forced to resist further stretching with a smaller area of sealant. Additionally, stress concentrations were created around the hole where the sealant initially ripped. These regions also began to slowly tear longitudinally, eventually ripping the entire cross sectional area (resulting in a cohesive failure).

The most common failure mode of the solid sealant involved a sudden adhesive failure, characterized by a detachment of the sealant from the substrate. Typically, the sealant detached at one edge of the substrate block and followed through the entire surface area. This indicated that upon an initial detachment, the remaining area of sealant in contact with the substrate block could not handle the added stress and released from the block. Figures 31-34 show the ultimate stress (stress at failure) for all specimens.

One of the most important factors included in this study was the effect of accelerated aging on the modulus of each sealant. Figures 35-38 show the modulus, stress at 100% strain (which is a common property when assessing the strength of the sealant, since a 100% extension of a joint gap can occur on a bridge).

Figure 31 shows the ultimate stress values for specimens exposed to salt and primer treatment. It can be observed that, over the span of 150 days, the stress at failure for both the foam and solid sealants reduced, indicating a possible reduction in modulus. This may be attributed to the salt deteriorating the bond between the sealant and the substrate blocks. Overall, the foam sealant's ultimate stress values were more consistent, whereas

the solid sealant exhibited a large range of failure stresses. This may be due to the higher stresses exerted on the interface of the solid sealant, which exposes any weak points or imperfections in the sealant.

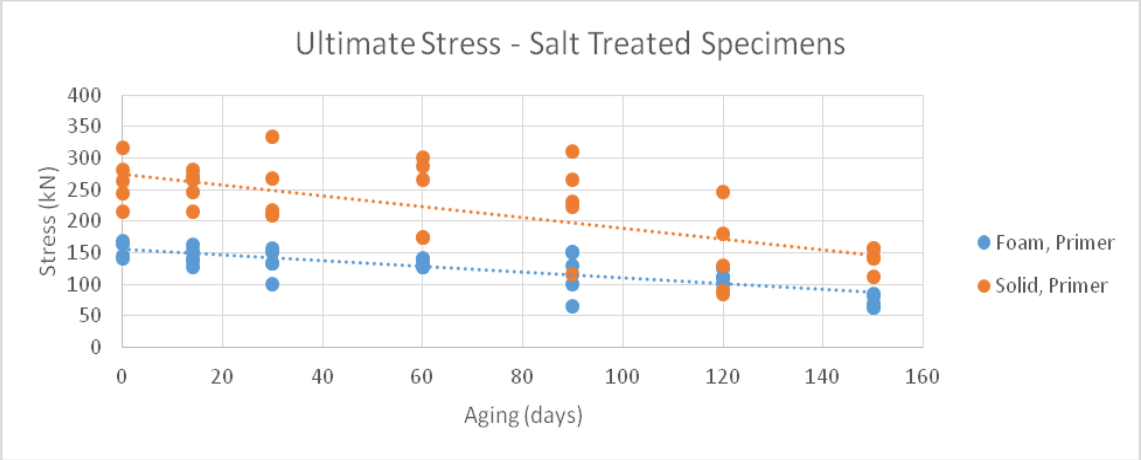

Figure 31: Ultimate stress for specimens exposed to salt with primer treatment

Figure 32 shows the ultimate stress values for specimens exposed to salt but no application of primer. Again, it can be observed that the stress at failure for both the foam and solid sealants reduced over the duration of the experiment. Judging from the trend line, the solid sealant's ultimate stresses appear to reduce at a faster rate than that of the foam sealant's, which may suggest that the effects of the salt and aging have more of an impact on the solid sealant.

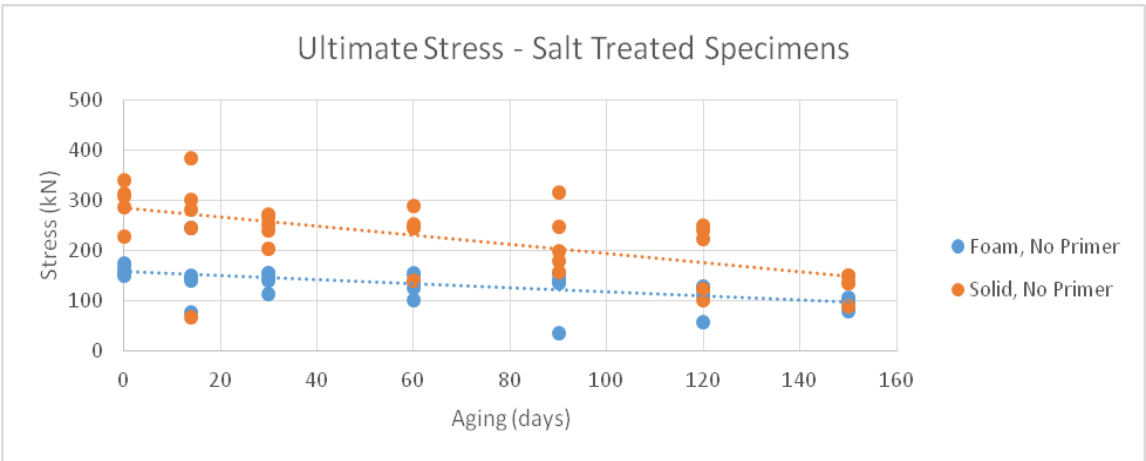

Figure 32: Ultimate stress for specimens exposed to salt without primer treatment

Figure 33 shows the ultimate stress values for specimens not exposed to salt but treated with primer. The ultimate failure stresses for the solid sealant is consistent with the other specimens at the start of the experiment (0 days), measuring approximately 280 kN. After 150 days of aging, the ultimate stress of the solid sealant measured consistently at approximately 140 kN, an overall reduction of about 50%. However, the foam

sealant's stress at failure dropped approximately 33% over the same time period and aging conditions.

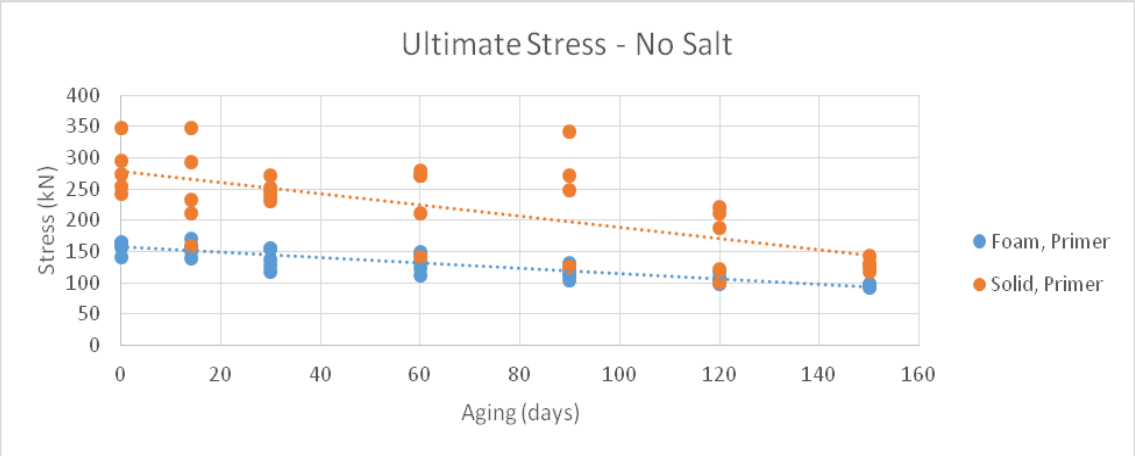

Figure 33: Ultimate stress for specimens not exposed to salt with primer treatment

Figure 34 shows the ultimate stress values for specimens not exposed to salt and also not treated with primer. The ultimate failure stresses are consistent with the previous results. Again, the solid sealant exhibits a sharper decline in tensile capacity, indicating its vulnerability to aging itself. At 0 days, the solid sealant's failure stress was (on average) approximately 290 kN, dropping to about 140 kN after 150 days of aging with no salt or primer. The foam sealant's capacity dropped from about 160 kN at 0 days to just below 100 kN after 150 days of aging.

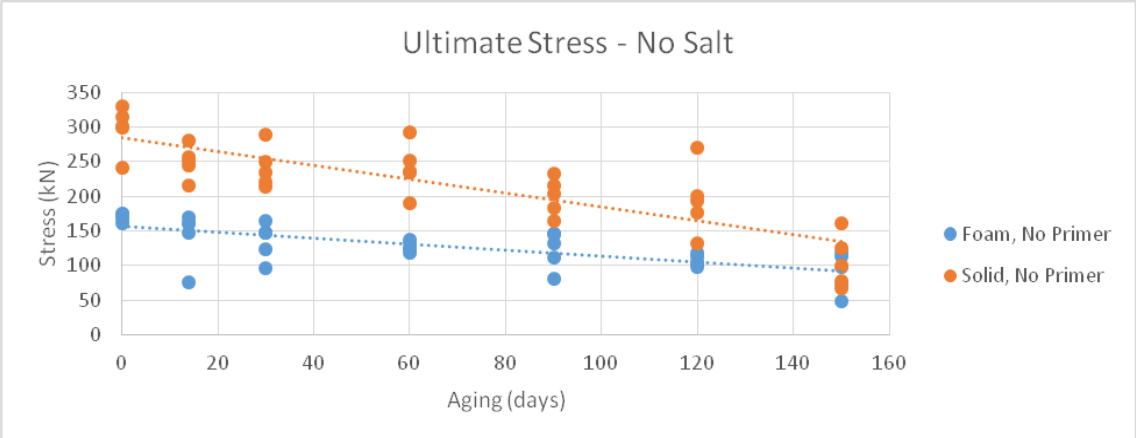

Figure 34: Ultimate stress for specimens not exposed to salt and with no primer treatment

From Figure 35, it can be observed that the modulus of the solid sealant decreases at a higher rate when exposed to salt water aging. The stress at 100% strain of specimens containing primer at 0 days (no aging) was measured to be approximately 39 kN. Over an aging period of 5 months, however, the stress dropped to about 21.5 kN, a reduction of 44.9%. The foam sealant, however, exhibited a more consistent modulus throughout the course of aging. The initial stress at 100% strain was observed to be about 26.9 kN,

dropping to about 21 kN after 5 months aging. This represents a reduction in stress of approximately 21.9%.

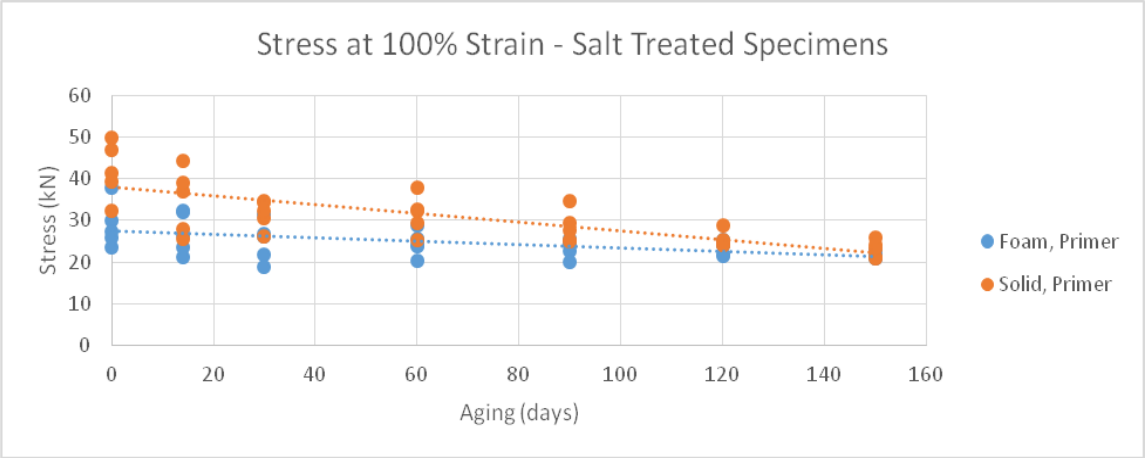

Figure 35: Stress at 100% strain for specimens exposed to salt and primer treatment

Figure 36 shows the behavior of the stress at 100% strain observed in specimens that were aged in the salt water tank, but did not receive primer treatment prior to immersion. Once again, the modulus of the solid sealant appears to decrease at a higher rate than that of the foam sealant. The stress at 100% strain of specimens containing primer at 0 days (no aging) was measured to be approximately 39 kN. Over an aging period of 5 months, the stress dropped to about 21 kN, a reduction of 46.1%. The foam sealant also exhibited a decrease in stress, but not as sharp as the solid sealant. The foam sealant's initial stress at 100% strain was observed to be about 27 kN, dropping to about 23 kN after 5 months aging. This represents a reduction in stress of approximately 14.8%.

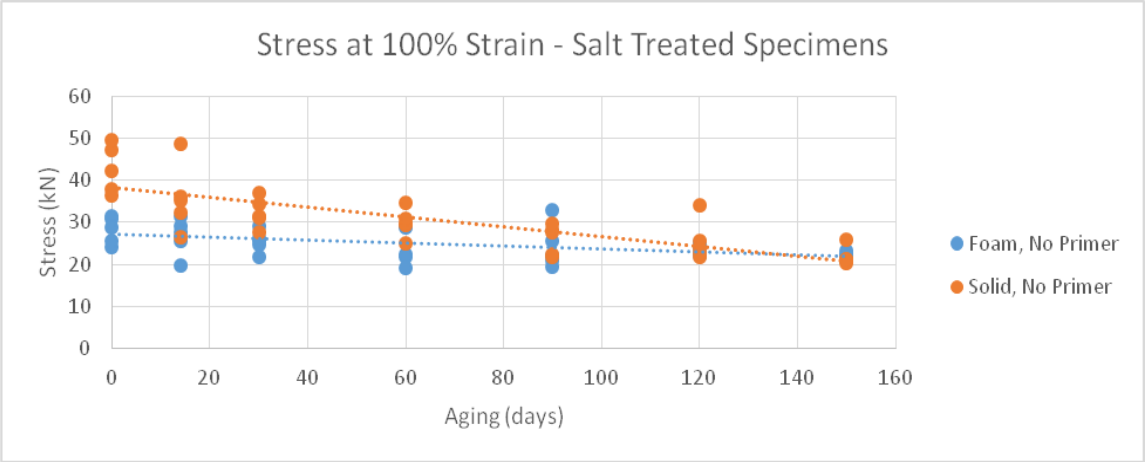

Figure 36: Stress at 100% strain for specimens exposed to salt without primer treatment

Figure 37 also shows that the modulus of the solid sealant appears to decrease at a higher rate than that of the foam sealant, even without the presence of salt. The stress at 100% strain of specimens containing primer at 0 days (no aging) was measured to be approximately 40.1 kN. Over an aging period of 5 months, however, the stress dropped to

about 23.5 kN, a reduction of 41.4%. The foam sealant, however, exhibited a more consistent modulus throughout the course of aging. The initial stress at 100% strain was observed to be about 26.9 kN, dropping to about 21 kN after 5 months aging. This represents a reduction in stress of approximately 21.9%.

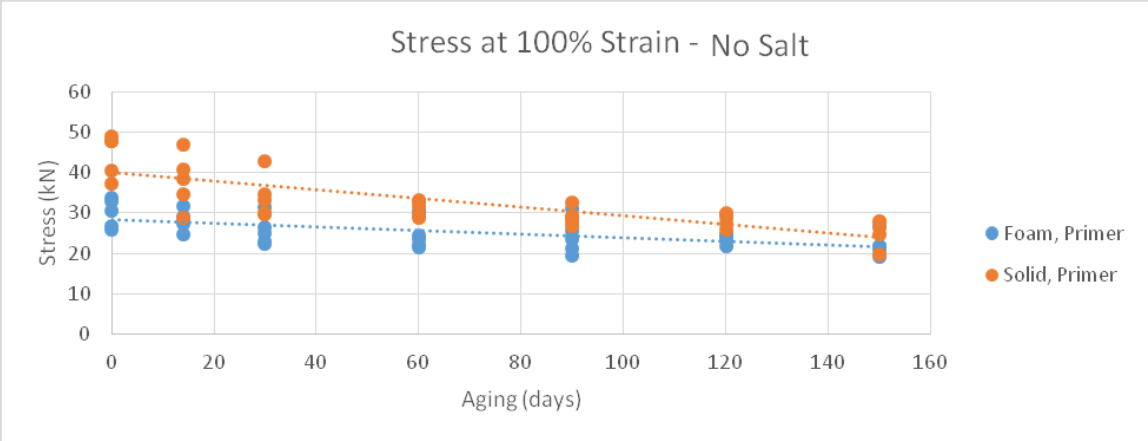

Figure 37: Stress at 100% strain for specimens not exposed to salt and with primer treatment

Figure 38 shows the stress at 100% strain for specimens not exposed to salt or treated with primer. Again, it can be observed that the stress at 100% strain drastically reduces after 150 days of aging, even to the point where the foam and solid stresses at 100% strain are almost equal at 150 days. Although the foam sealant also exhibits a reduction in stress at 100% strain as a function of aging, the drop is not as significant.

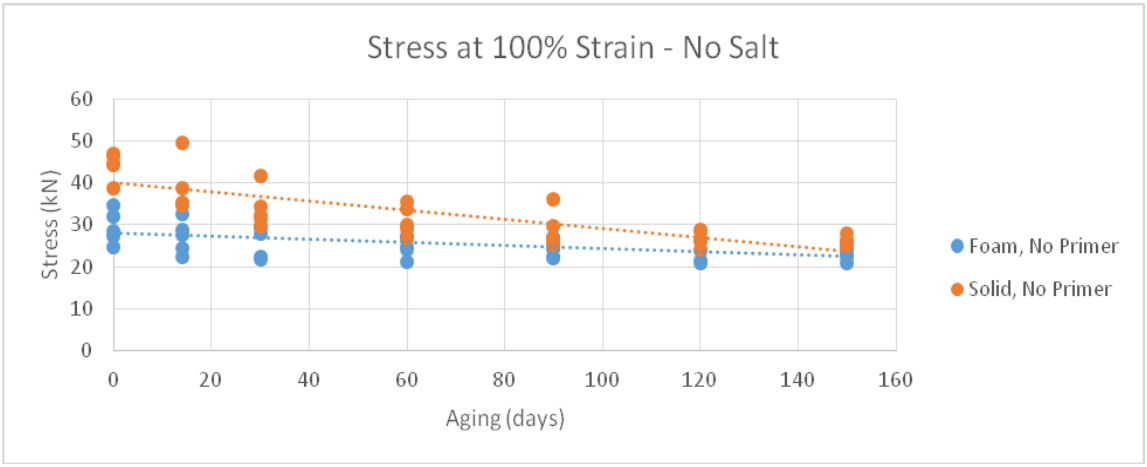

Figure 38: Stress at 100% Strain for specimens not exposed to salt and with no primer treatment

Figure 39 shows the ultimate elongation of the specimens treated with salt, but not with primer. It can be observed that the average elongation for the solid sealant appears to be almost the same over time, judging by the trendline. However, the foam sealant's elongation tends to increase over time, possibly suggesting a reduction in stiffness (and therefore an increase in ductility).

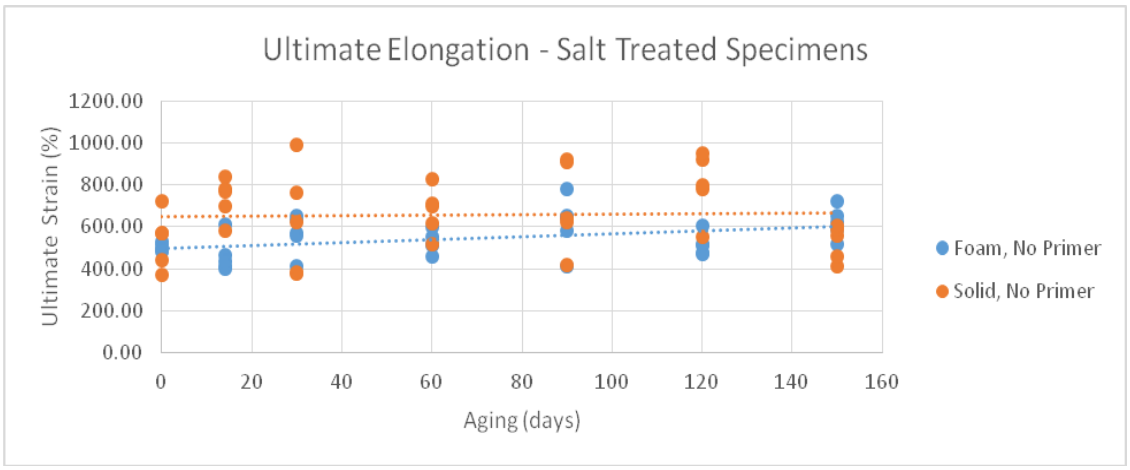

Figure 39: Ultimate strain (elongation) for specimens exposed to salt without primer treatment

Figure 40 also shows the ultimate elongation for salt treated specimens that received primer treatment to the substrate. Although the initial few elongations are rather scattered, both sealants show a more consistent elongation at failure towards the longer aging durations (90, 120 and 150 days). This result may suggest that the deteriorative effects of the salt may affect both sealants in a similar fashion, resulting in more consistent failure strains.

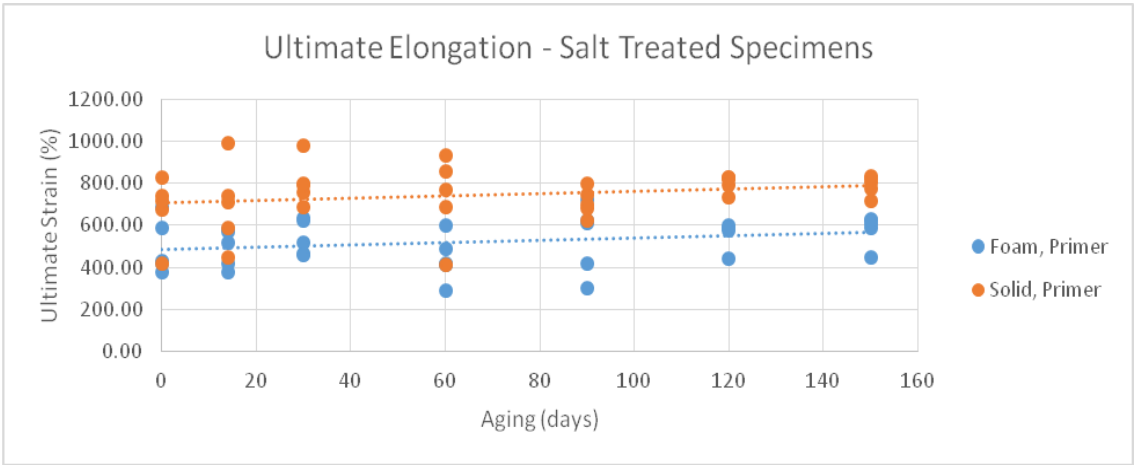

Figure 40: Ultimate strain (elongation) for specimens exposed to salt with primer treatment

Figure 41 shows the ultimate elongation for specimens not exposed to salt or primer. Again, the elongations are rather scattered due to imperfections in the material, casting, and a small coupon size. However, the general trend suggests that both sealants exhibit a fairly consistent ultimate elongation, with a slight increase over a duration of 150 days.

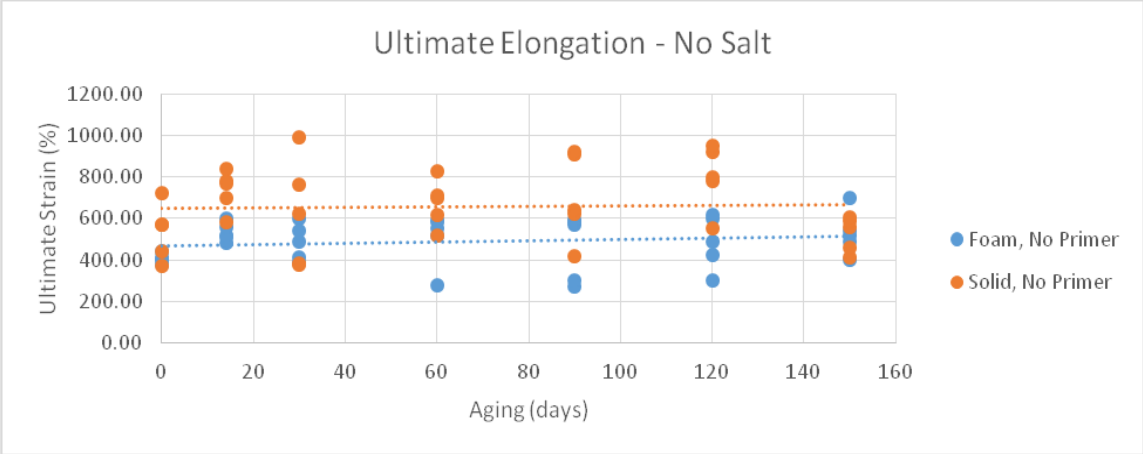

Figure 41: Ultimate strain (elongation) for specimens not exposed to salt and with no primer treatment

Figure 42 shows the ultimate elongation for specimens not exposed to salt but treated with primer. The initial elongation of the foam specimens are relatively low compared to the other specimens (most likely due to the one specimen that failed at less than 200% elongation due to some weakness in the material). However, the general trend shows that the foam exhibits a larger elongation over the duration of aging, whereas the solid sealants elongation stays approximately the same.

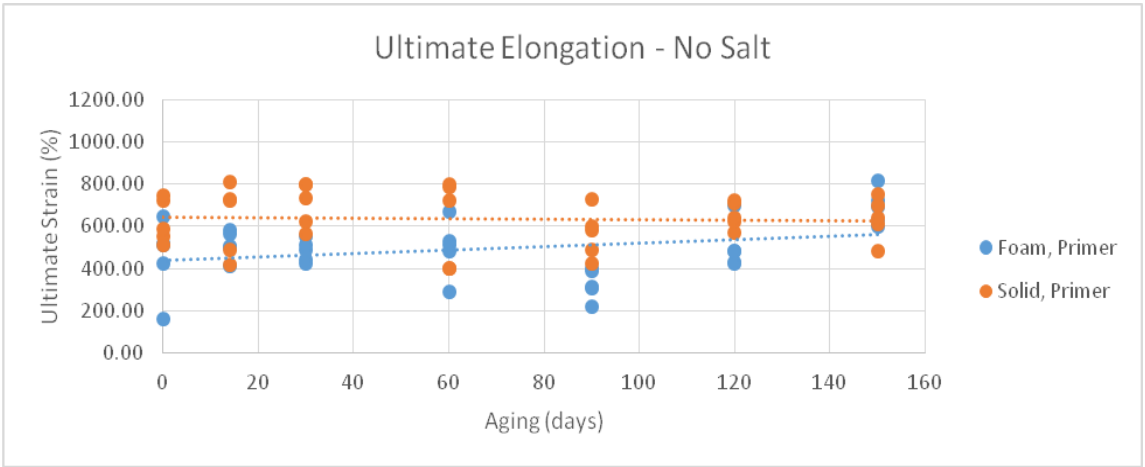

Figure 42: Ultimate strain (elongation) for specimens not exposed to salt and with primer treatment

Tables 4 and 5 show the average ultimate stress, average ultimate strain, and adhesive failure fraction for all specimens as a function of aging. Five specimens were tested for each parameter (i.e., five specimens containing foam sealant with primer at 0 days' duration, and another five specimens containing foam sealant without primer for the same aging period). The average values reflect the measured average of all five specimens for that particular parameter. The ultimate stress for each specimen was recorded when the sealant could no longer sustain a higher load, regardless of continuous deformation. The ultimate strain for each specimen was considered as the maximum sustained strain before complete detachment from the substrate or the sealant itself.

Table 4: Saltwater aging test – average ultimate stresses and strains (salt treated specimens)

Salt Treated Specimens					
Age (days)	**Sealant Type**	**Surface Prep**	**Average Ultimate Stress (kPa)**	**Average Ultimate Strain (%)**	**Adhesive Failure Mode (%)**
0	Foam	Primer	157[a] ± 9.6[b]	501 ± 130.7	20
		No Primer	159 ± 8.2	504 ± 20.74	20
	Solid	Primer	264 ± 30.6	676 ± 154	100
		No Primer	295 ± 33.4	679 ± 90.58	100
14	Foam	Primer	144 ± 11	493 ± 91.9	20
		No Primer	152 ± 48	464 ± 85.4	0
	Solid	Primer	256 ± 21.2	695 ± 200.9	100
		No Primer	255 ± 94	522 ± 159.2	100
30	Foam	Primer	135 ± 17.8	539 ± 83.6	20
		No Primer	141 ± 13.2	565 ± 95.1	0
	Solid	Primer	248 ± 43.2	803 ± 108.7	100
		No Primer	247 ± 21.6	380 ± 117.2	100
60	Foam	Primer	134 ± 5	443 ± 113.5	0
		No Primer	134 ± 17.6	528 ± 51.6	0
	Solid	Primer	240 ± 49.4	730 ± 200.8	100
		No Primer	234 ± 44.8	731 ± 200.7	80
90	Foam	Primer	119 ± 29.8	534 ± 169.9	0
		No Primer	120 ± 38.4	614 ± 132.8	0
	Solid	Primer	229 ± 58	709 ± 67.8	80
		No Primer	219 ± 50.2	485 ± 67.6	80
120	Foam	Primer	115 ± 8.8	558 ± 66.5	0
		No Primer	109 ± 24.2	516 ± 54.2	0
	Solid	Primer	146 ± 54.4	800 ± 39.5	60
		No Primer	187 ± 55.8	527 ± 193.9	80
150	Foam	Primer	72 ± 7.8	579 ± 74.0	0
		No Primer	95 ± 9	621 ± 73.8	0
	Solid	Primer	142 ± 14	790 ± 47.4	80
		No Primer	131 ± 19.4	751 ± 95.8	80

[a]Average of five samples tested (complete specimen information found in Appendix A)
[b] 95% confidence interval for the average

Table 5: Saltwater aging test – average ultimate stresses and strains (non-salt treated specimens)

Non-Salt Treated Specimens					
Age (days)	**Sealant Type**	**Surface Prep**	**Average Ultimate Stress (kPa)**	**Average Ultimate Strain (%)**	**Adhesive Failure Mode (%)**
0	Foam	Primer	158[a] ±7.6[b]	451 ± 180.6	0
		No Primer	170 ±4	407 ± 22.2	20
	Solid	Primer	282 ±33.2	623 ± 105	100
		No Primer	297 ±27	534 ± 135.1	100
14	Foam	Primer	154 ±9	512 ± 66.9	0
		No Primer	143 ±30.8	534 ± 46.6	20
	Solid	Primer	248 ±58.4	634 ± 168.9	100
		No Primer	249 ±19	734 ± 99.4	100
30	Foam	Primer	138 ±13	483 ± 51.1	0
		No Primer	136 ±21.2	486 ± 87.9	0
	Solid	Primer	247 ±12	702 ± 105.2	100
		No Primer	241 ±23.8	629 ± 259.9	100
60	Foam	Primer	133 ±12.4	496 ± 136.3	0
		No Primer	127 ±6.2	505 ± 128.9	0
	Solid	Primer	235 ±47.2	621 ± 203.8	100
		No Primer	241 ±29.6	674 ± 117.3	100
90	Foam	Primer	116±8	325 ± 73.31	0
		No Primer	123 ±21.8	463 ± 163.0	0
	Solid	Primer	222 ±75.8	565 ± 116.0	100
		No Primer	199 ±21.2	702 ± 213.0	100
120	Foam	Primer	105 ±2	504 ± 112.9	0
		No Primer	107 ±6.4	485 ± 130.8	0
	Solid	Primer	168 ±43.6	653 ± 62.4	80
		No Primer	194 ±40.2	800 ± 157.9	100
150	Foam	Primer	95 ±1.8	691 ± 83.9	0
		No Primer	90 ±23.2	530 ± 109.1	0
	Solid	Primer	128 ±7.6	636 ± 102.6	80
		No Primer	106 ±30.2	525 ± 85.6	80

[a]Average of five samples tested
[b] 95% confidence interval for the average

In order to investigate the effect of each individual parameter (salt, primer application, foam, and age) on the ultimate stress, ultimate strain, stress at 100% strain and adhesive failure fraction, a multi-parameter linear model was applied to the entire

data set using PSI-Plot (PSI-Plot 2015). In spite of being linear, a non-linear fitting method, the Levenberg-Maquardt LSQ method (Lourakis 2005), was used as the software was more convenient. Each parameter that influenced the specimens was assigned a variable, which was multiplied by a "parameter term" which defines how significant that parameter is. Variables such as x_1, x_2, x_3, and x_4 were used for salt, primer, foam, and age, respectively. All results were tabulated according to age and each specimen was coded using a binary system. For example, a specimen containing foam exposed to salt, aging, and primer application would be identified as $x_1 = 1$, $x_2 = 1$, $x_3 = 1$, and x_4 ranging from -3 to 3 to define all seven aging periods. The aging parameter was set from -3 to 3, so that the model would intercept 0 at 2 months aging. When solid sealant was used, x_3 was set to 0. This terminology allowed for including the global effect of all parameters when using the fitting model, shown below.

$$y = a_0 + a_1x_1 + a_2x_2 + a_3x_3 + a_4x_4 + a_{12}x_1x_2 + a_{13}x_1x_3 + a_{14}x_1x_4 + a_{23}x_2x_3 + a_{24}x_2x_4 + a_{34}x_3x_4 \quad (2)$$

The model also included terms for interaction between two or more parameters, since specimens exposed to salt and age may have performed differently than specimens exposed to just aging. These parameters, for example, are defined by x_{12}, which would represent the interaction between salt and primer application. The parameter values, labeled as a_0, a_1, etc., were generated once the model was run. All parameter and interaction terms are defined in Table 6.

Table 6: Parameter and interaction terms for LSQ model

Variable	Parameter	Interaction
x_1	Salt	--
x_2	Primer	--
x_3	Sealant	--
x_4	Age	--
a_{12}	--	Salt and Primer
a_{13}	--	Salt and Sealant
a_{14}	--	Salt and Age
a_{23}	--	Primer and Sealant
a_{24}	--	Primer and Age
a_{34}	--	Sealant and Age

The model provided parameters values and invariant 95% confidence intervals, which were used to generate p-values. These p-values indicate the probability of error in rejecting the null hypothesis, i.e., the factor (aging time, salt concentration, etc.) is not significant. P-values less than 0.05 were considered to be an acceptable threshold of reliability for this study.

As expected, the specimens with foam sealant instead of solid sealant had a significant influence on the reduction of ultimate stress, yielding a p-value of less than 0.001 (t = 16.20). Likewise, the model showed that age also had a statistically significant influence on the reduction of the ultimate stress, yielding a p-value less than 0.001 (t = 14.09). The interaction between these two parameters (foam and age) confirmed these conclusions, as the yielded p-value was also less than 0.001 (t = 6.23). Interestingly, the interaction between salt and primer yielded a p-value of 0.008 (t = 2.73), which may suggest a deteriorative property of these two parameters on the ultimate stress.

Due to large variations in the ultimate strains, the statistical analysis for ultimate strain only yielded a significance when foam specimens were tested, which is expected (p-value generated was less than 0.001 and the t-value was 4.74). When considering the adhesive failure fraction, which is the fraction of adhesive failures (clean detachment from the substrate), out of five specimens tested for a particular parameter, several parameters generated a statistically meaningful effect. The inclusion of salt generated a p-value of 0.0013 (t = 3.41), indicating that the effect of salt may have an effect on the bond between the sealant and the substrate. However, when examining the effect of primer on the failure fraction, the yielded p-value was 0.79 (t = 0.25), suggesting that the effect of primer on the bond is likely to be small. Interestingly, the interaction between salt and primer generated a p-value of 0.054 (t = 1.97), which is slightly higher than the acceptable threshold to draw a reasonable conclusion. However, this result suggests a possible deteriorative effect due to a combination of salt and primer application. Additionally, the model results suggest that the effect of aging time has a statistically significant effect on the adhesive failure fraction, generating a p-value of 0.003 (t = 3.88).

2.9 Volume Expansion Test and Results

Previous studies conducted by Malla, et al., (2007) have indicated that the foam sealant exhibits significant expansion after casting, often between 50% and 70%. To understand better the characteristics of expansion and determine the cause for such variations, the expansion experiment was established to examine the influence of initial volume of sealant on the total expansion. This concept was formulated from observations in the laboratory when certain specimens with varying amounts of sealant exhibited different expansion characteristics. Motivation to understand the behavior of expansion in this foam sealant stemmed from specifications for poured silicone sealant joints by Watson Bowman Acme, which suggest a 12.7 mm (0.5 in.) layer of silicone to be applied above the backer rod. The top surface of the silicone seal should also be recessed at 12.7 mm (0.5 in.) from the roadway. This is primarily to prevent damage to the joint itself due to repeated vehicular loading and reduce the likelihood of snow plows tearing the sealant. Since the foam sealant exhibits significant expansion upon initial set, understanding the behavior of the expansion would provide insight to the quantities needed to prevent expanding over the roadway and, instead, expand to the appropriate height above the backer rod.

In order to study the expansion as a function of initial volume, the foam sealant was cast into forms resembling a small section of a typical small movement bridge joint. The

dimensions of each form were L = 152.4 mm (6 in.), W = 25.4 mm (1 in.) in, and D = 38.1 mm (1.5 in.) (Figure 43). As shown in Table 7, the initial thickness of sealant applied in each form ranged from ¼″ to 1″, representing typical minimum and maximum thickness of sealant that would be applied into an in-service bridge joint.

Table 7: Initial thicknesses of specimens for expansion test

Specimen No.	1	2	3	4	5	6	7	8	9	10
Specimen Thickness (mm)	3.18	3.97	7.94	7.94	7.14	7.94	9.53	11.91	12.70	13.49

The thickness of each joint was measured every minute for the first 20 minutes after initial casting, and then, every 5 minutes until the sealant exhibited no further expansion for three consecutive measurements. A laser-based distance measurement device was used to measure the thickness of the sealant at each time interval. The device was placed two inches above each set of blocks in order to ensure a consistent reference point for each specimen. A schematic of the experimental set up is shown in Figure 43.

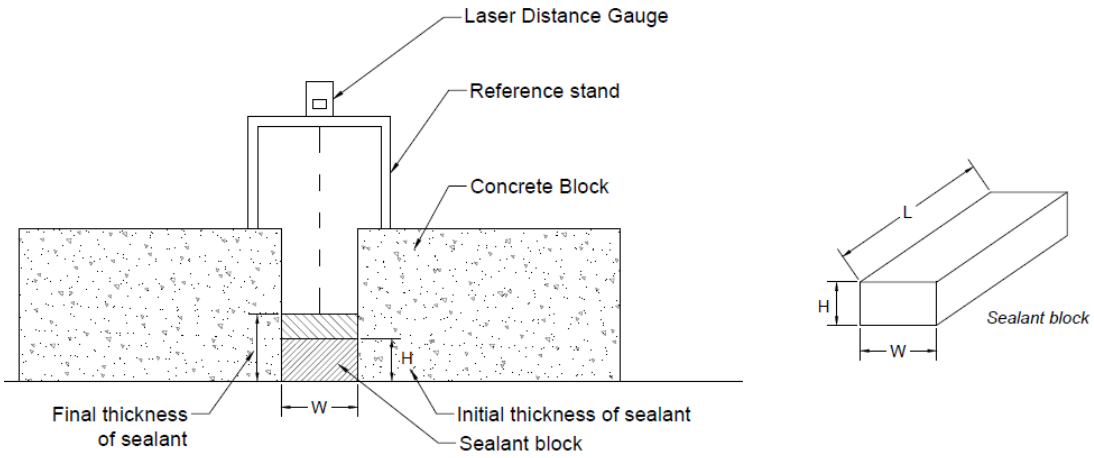

Figure 43: Expansion test assembly

As shown in Figure 44, the initial volume of sealant applied directly correlates to the final thickness of the sealant. For example, an initial thickness of 0.25″ produced a final thickness of 0.375″, while an initial thickness of 1″ produced a final thickness of almost 1.75″. The total exact expansions for these particular trials were 50% and 74%, respectively. The difference in expansion from one specimen to another may stem from greater amounts of hydrogen gas being lost from the specimen containing less sealant. Additionally, it can be observed that specimens containing a smaller initial amount of sealant experienced slower expansion in a step-like manner. The specimens containing a thicker amount of sealant expanded more rapidly over time with larger and more frequent steps.

These results indicate that applying the appropriate initial thickness of sealant into an expansion joint is crucial to ensure no sealant expands over the top edge of the substrate. Moreover, care must be taken to avoid applying conservative amounts of sealant as this

may results in too thin of a layer of sealant. If the joint is too thin, it may puncture or allow water/debris to penetrate through to the substructure.

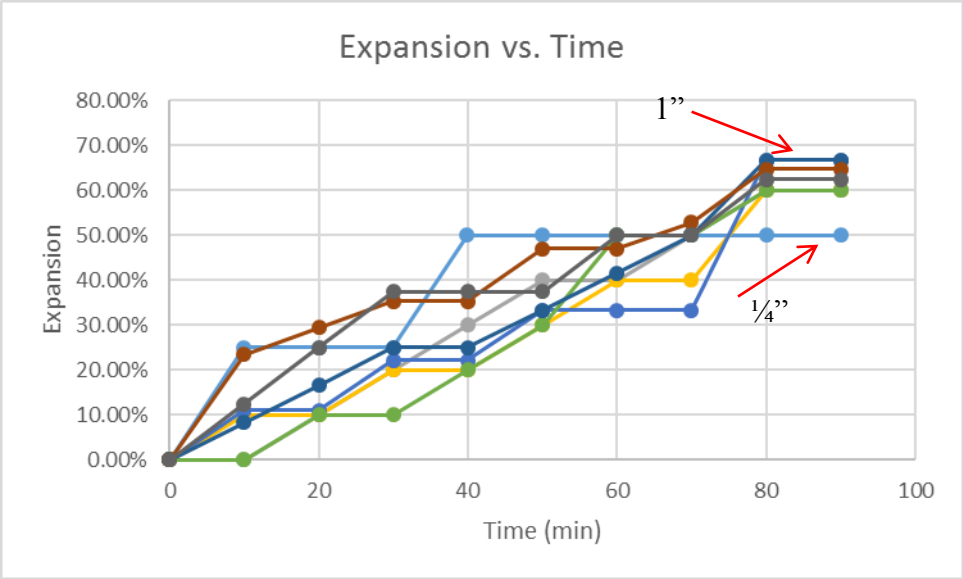

Figure 44: Expansion vs. time for foam sealant

3.0 FIELD INSTALLATION

Through the coordination of CT DOT, experimental expansion joints were installed on three bridges throughout the state of Connecticut. Each bridge was chosen appropriately so that the foam sealant could accommodate the induced movements. Traffic volume was an important factor in the choices.

3.1 Route 6 Bridge

The Route 6 bridge is located in Windham, CT. It features two 170-ft. spans over the Route 6 expressway. Although the bridge spans over Route 6, vehicles travel under the bridge as part of Route 6 and circle around to travel on the bridge itself, still as part of Route 6 (Figure 45). This 8-girder composite bridge contains a steel girder superstructure and a 7.75-inch concrete road deck with concrete joint headers (Figure 46). A 2.5-inch bituminous concrete wearing surface and waterproofing membrane rest on top of the concrete deck. According to the 2013 Bridge Safety Inspection report, the average daily traffic (ADT) for this bridge is 15,700 vehicles. The bearings are fixed at the pier, so each abutment joint accommodates movement over a temperature range of −10 °F to 110 °F, resulting in a theoretical movement of each joint of approximately 1.53 inches as per AASHTO specifications (AASHTO 2012). The speed limit on the bridge is 45 miles per hour. The state of Connecticut previously installed a silicone sealant which failed after an unknown period of time. Typically, they would install an asphaltic plug joint (APJ) to repair joints of this nature; however, the total movement of this bridge exceeds the capabilities of the asphaltic plug joint. Therefore, the silicone foam sealant joint was a good candidate for this bridge.

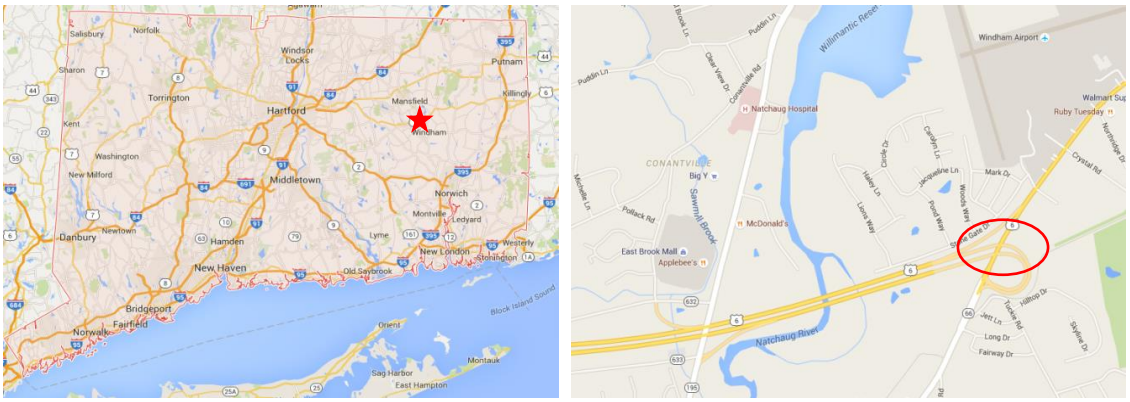

Figure 45: Map location of the Route 6 Bridge in Windham, CT

(a) (b)

Figure 46: Route 6 Bridge (a) Span and center pier, (b) support at abutment

The full width of the bridge deck joint was sealed, amounting to a total of 106 feet (53 feet per joint). At the time of installation, the west joint had an average gap opening of 1.75 inches and the east joint had an average gap opening of 1.5 inches. However, due to imperfections of the concrete header, the gap width varied along the length of the joint by ± 0.25 inches.

The installation of the sealant into the expansion joints of the Route 6 bridge was a two-day operation, conducted on Monday and Tuesday, September 14-15, 2015. The sealants for lane 1 and the south shoulder (shown in Figure 47) were installed on Monday, September 14. Weather conditions for Monday were mostly sunny with some scattered clouds with a high temperature of 76 °F. Roadway temperatures and air humidity for this day ranged between 83-97 °F and 18-26%, respectively. The sealants for lanes 2, 3 and the north shoulder were installed on Tuesday, September 15, 2015. Weather conditions for Tuesday were mostly sunny with some scattered clouds with a high temperature of 80 °F. Roadway temperatures and air humidity for this day ranged between 92-105 °F and 16-22%, respectively.

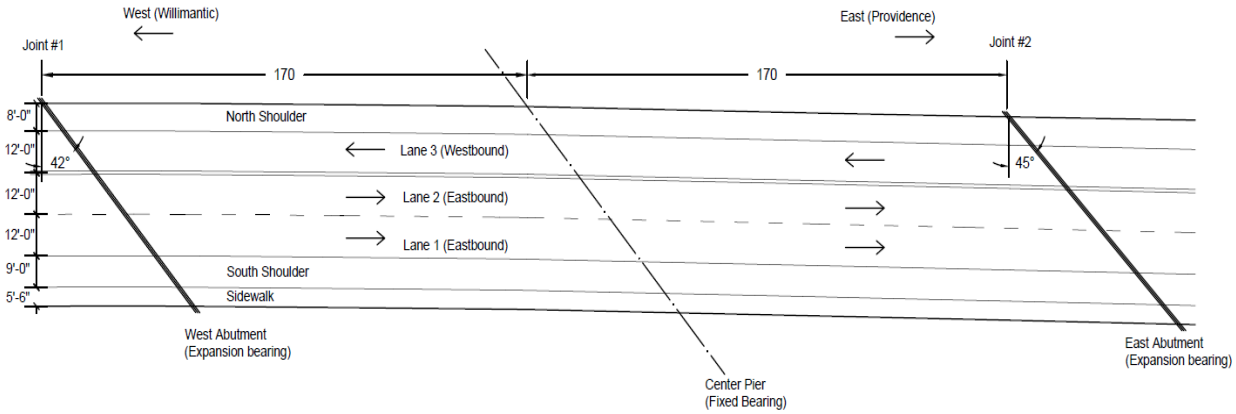

Figure 47: Plan schematic of Route 6 Bridge

The preparation of the joint (Figure 48) prior to actual installation of the sealant involved removing the existing joint and sand blasting the header to ensure any remnants

of the previous joint were removed. Since this particular bridge was sealed using a poured silicone joint in the past, care was taken to ensure no remnants of the silicone joint were remaining on the substrate. This was to optimize the bond between the new foam sealant and the substrate. Once the surface was free of any loose material, a rag was used to apply a thin coating of acetone to the header of the bridge to remove any oils that may be present on the surface of the header.

Figure 48: Sand blasting and primer application onto the Route 6 Bridge joint

First, the entire joint was cleaned by thoroughly sandblasting the header to remove any sand or debris that may have been carried into the joint (Figure 48). Next, the entire header surface was cleaned using a rough rag and acetone, resulting in a clean and oil-free header surface (Figure 49a). The top surface of the joint header close to the joint gap was covered with duct tape to prevent any silicone from sticking to the roadway. This also allowed for a clean termination line between the edge of the substrate and the silicone sealant. A 3-inch diameter backer rod was inserted one inch below the surface of the road using a T-shaped spacing tool (Figure 49b). The vertical portion of the spacing tool was exactly one inch, which allowed for a consistent recess of the backer rod along the joint. The backer rod was a 3-inch diameter closed cell, polyethylene extruded foam rod, with excellent UV and moisture resistance. Dividers were placed at the boundary sections (between the foam and solid sealant) to ensure the foam sealant did not spill over into the portion designated for solid sealant.

(a) (b)

Figure 49: Overview of the joint on Route 6 Bridge (a) before backer rod installation and (b) after installation

The placement of the sealants and the application of primer were chosen by following the Latin square method of systematically assigning variables to a field (Figure 50). This pattern was applied to one lane and, then, rotated clockwise for each adjacent lane to minimize bias of placement. It was assumed that any vehicle driving over the bridge stays in the same lane when it encounters both joints. This would allow for a straight forward comparison of the in-service behavior for the joint containing foam sealant with primer, foam sealant without primer, solid sealant with primer, and solid sealant without primer. Each lane was split into two sections per joint; therefore, all four variables were included in each joint. It was assumed that the effect of the left tire onto the joint was the same as the effect of the right tire. Therefore, the effectiveness of the primer and the foam sealant could be easily observed when assessing each section of the lane.

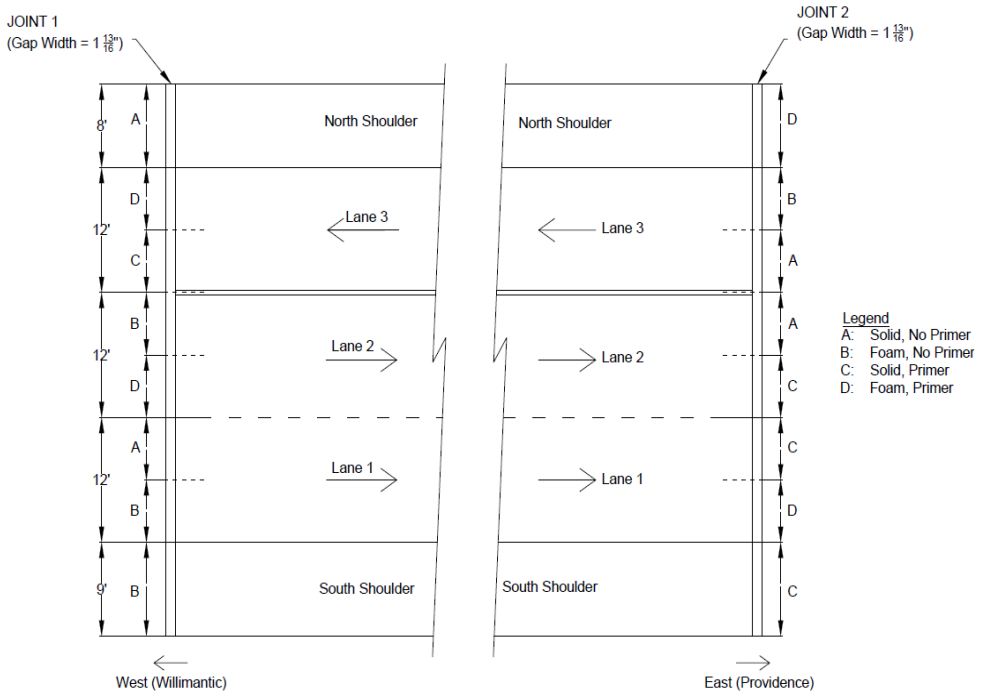

Figure 50: Sealant and primer placement plan, Route 6 Bridge

Once the entire joint was prepared for pouring, appropriate amounts of each component were mixed to create the foam sealant formulation. Knowing the joint gap and sections of sealant needed, as indicated in the placement plan, the components were pre weighed for lengths equivalent to half of a lane. Each component was sealed and stored in labeled syringes to facilitate the mixing process in the field without having to weigh out each component on site. Since the foam sealant is known to have a longer curing time, the foam sealant was placed first. The components were mixed on site in a bucket using a hand drill with an appropriate mixing attachment. Equal parts by volume of the Wabo white and Wabo (WBA 2008a) black were combined and mixed in a bucket using the hand drill. Once a uniform color was established, the platinum was slowly added while continuously stirring the sealant. The addition of water followed. Once these four components were thoroughly mixed, the crosslinker was also added while continuously stirring the sealant. After a uniform texture was obtained, the sealant was carefully

poured into the joint manually, from the bucket where the sealant components were mixed together (Figure 51). The sealants were installed section-by-section, as outlined in the plan shown in Figure 50. A leveling tool, also T-shaped, was used to establish the appropriate recess from the roadway. The vertical portion of the T was exactly 0.5 inches in height, so the sealant was poured and shaped with a recess of 0.5 inches from the surface of the road.

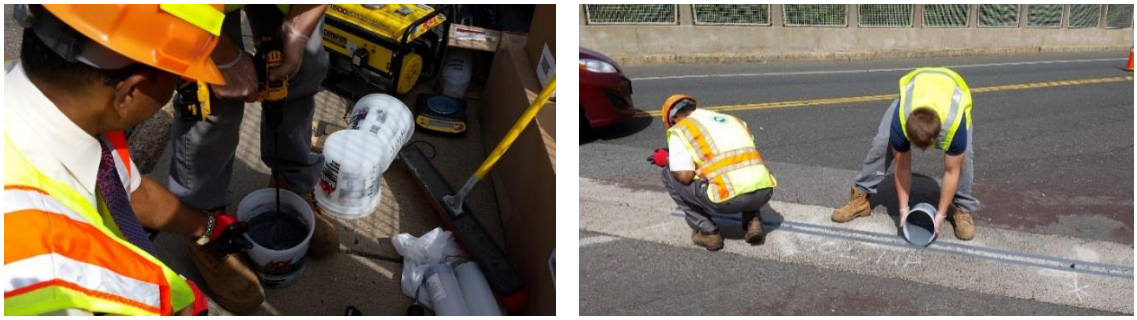

Figure 51: Installation of the sealant, Route 6 Bridge

The details of the sealant installation were meticulously recorded, as the curing of the sealant was time-dependent. Tack free time for the foam sealant is approximately 1.5 hours, while tack free time for the solid sealant is about 1 hour. However, these times are highly dependent on the outside temperature and humidity. Silicone tends to cure quicker with higher temperatures. This difference in curing time motivated the group to install the foam sealant prior to installing the solid sealant at each lane. The average time for mixing, pouring and leveling one lane was approximately 35 minutes (both joints).

3.2 Route 291 Bridge

The Route 291 Bridge is located in Windsor, CT, as part of Route 291, spanning Deerfield Road (Figure 52). The structure is a four-span continuous, curved, multi-girder steel bridge carrying four lanes of traffic (two in each direction). This 9-girder composite bridge contains a steel-girder superstructure, an 8.25-inch concrete road deck, and a 2.5-inch wearing surface with a waterproof membrane. The joint headers are concrete. According to the 2014 Bridge Safety Inspection report by CT DOT, the anticipated daily traffic (ADT) for this bridge is about 52,600. The structure is supported at each abutment, and at three intermediate piers spaced at 132, 124, 124, and 124 feet, from west to east. The middle pier (pier 2) is fixed, while the exterior piers and abutments contain rollers to accommodate expansion. Figure 53 shows the schematic of the bridge. Each abutment joint accommodates movement over a temperature range of −10 °F to 110 °F, resulting in a theoretical movement of each joint of approximately 2.44 inches, as per AASHTO specifications. The speed limit on this bridge is 65 miles per hour. The state of Connecticut previously installed a poured silicone sealant joint which failed after two full years. This bridge was a good candidate to directly compare the longevity of the foam sealant in comparison to the previously-installed, commercially-available product.

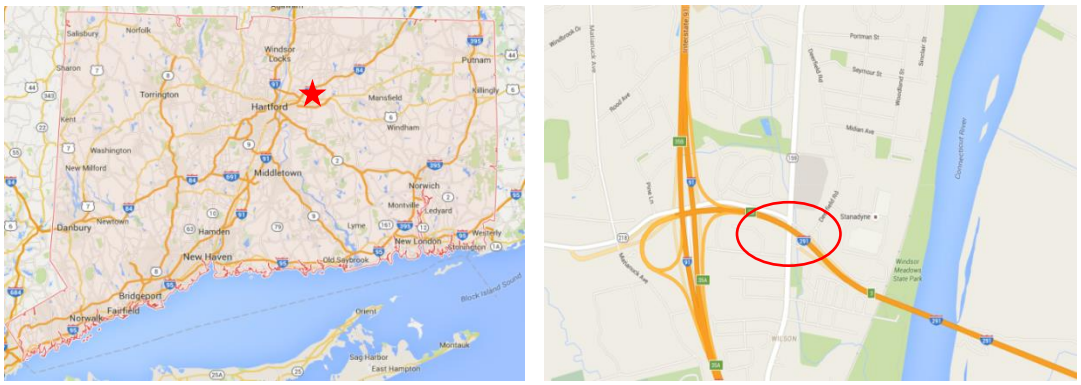

Figure 52: Location of the Route 291 candidate bridge

Three joints, all located on the east-bound portion of the highway, were sealed on this bridge; two expansion joints at each abutment, and one static joint parallel to the west side joint. The static joint was included into the structure of the bridge when repairs were conducted in the past. The average width of the static joint is approximately 1″ along the entire length. Since the bridge experienced some repair work in the past, the gaps were not a uniform width along the length of the joint. The west side joint gap varied between 3.125 – 3.375 inches. The west side joint gap varied between 2.625 – 3.5625 inches. The total length of expansion joints to be sealed amounted to 114 feet (3 joints of 38 feet each), as only the east-bound portion of the highway was sealed; the west-bound portion of the highway was not sealed.

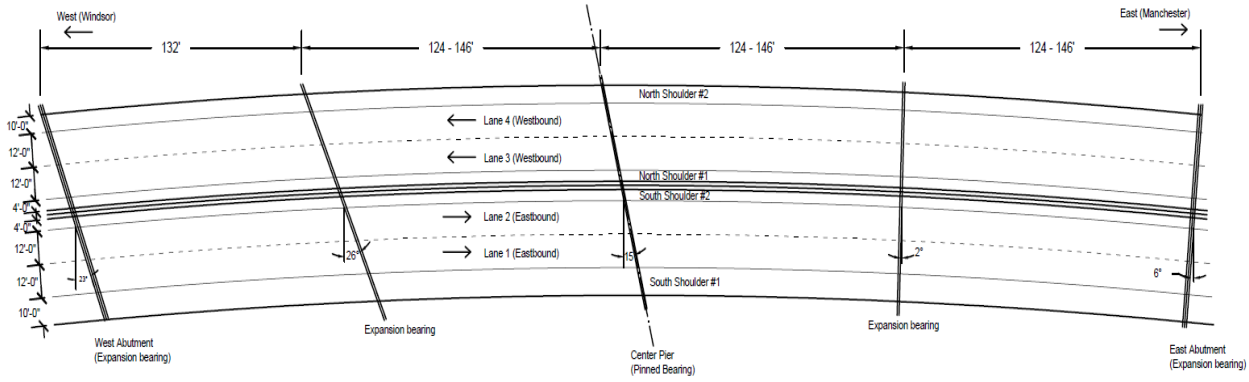

Figure 53: Plan schematic of Route 291 Bridge

The installation of the expansion joints of the Route 291 bridge was a three-day operation; CT DOT provided conservative installation time gaps due to the importance of the route for commuters and its high traffic volume. The installation was conducted on Monday, Tuesday and Thursday, October 5, 6, and 8, 2015. Weather conditions for Monday, October 5, were mostly sunny with some scattered clouds and a high temperature of 60 °F. Roadway temperatures and air humidity at time of installation ranged between 71-77 °F and 37-44%, respectively. Weather conditions for Tuesday, October 6, were mostly sunny with some scattered clouds and a high temperature of 66 °F. Roadway temperatures and air humidity at time of installation ranged between 70-86

°F and 29-41%, respectively. Weather conditions for Thursday, October 8, were mostly sunny with some clouds and a high temperature of 72 °F. Roadway temperatures and air humidity at time of installation ranged between 64-70 °F and 51-63%, respectively.

The preparation of the joint, prior to installation of the sealant, involved removing the existing joint, which was coordinated by CT DOT as a night job conducted prior to installing the new expansion joint. This was done to save time and avoid disrupting traffic on the day of installation. The header was thoroughly sand-blasted to remove any loose material and remnants of the old joint. Additionally, a large blade saw was applied to the header to cut into the concrete and expose a fresh surface for optimal bond (Figure 54). Dividers were placed at the boundary sections (between the foam and solid sealant) to ensure the foam sealant did not spill over into the portion designated for solid sealant. Finally, an acetone-soaked rag was used to remove any oils that may have potentially been left on the surface.

Figure 54: Joint preparation on Route 291 Bridge

Next, the top surface of the joint header was lined with duct tape to prevent any silicone from sticking to the roadway. A 5-inch backer rod was inserted one inch below the surface of the road using a T-shaped spacing tool (Figure 55). The vertical portion of the spacing tool was exactly one inch, which allowed for a consistent recess of the backer rod along the joint. The backer rod was a 5-inch diameter closed cell, polyethylene extruded foam rod with excellent UV and moisture resistance. The joint was air blown after installation of the backer rod to remove any sand or debris that may have been carried into the joint after initial cleaning.

Figure 55: Installation of backer rod and duct tape lining, Route 291 Bridge

After cleaning the joint from any loose debris or oils, primer was applied in locations, as depicted in the sealant placing pattern shown in Figure 56. The application of the primer and placement of the sealants were again done following the Latin Square Method as done for Route 6 bridge joints above. Once the entire joint was prepared for sealant pouring, the foam and solid sealants were mixed and poured into the joint following the same procedure outlined in section 3.1

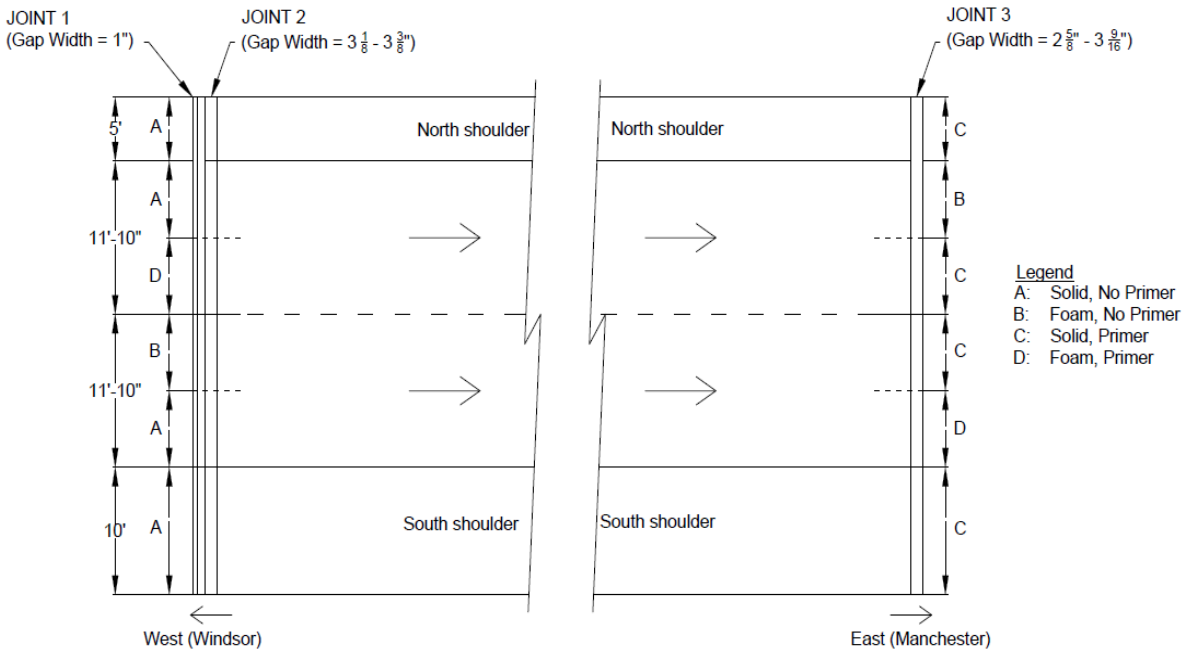

Figure 56: Sealant and primer placement plan, Route 291 Bridge

3.3 Route 22 Bridge

The Route 22 Bridge selected for field implementation in this project is located in North Haven, CT. It features two 141-ft. spans over Route 40 (Figure 57). This 5-girder composite bridge contains a steel girder superstructure and an 8-inch reinforced concrete deck (with concrete joint headers). A 2.5-inch bituminous concrete wearing surface and waterproofing membrane rest on top of the concrete deck. According to the 2013 Bridge Safety Inspection report, the anticipated daily traffic (ADT) for this bridge is 6,100 vehicles. The bearings are fixed at the center pier, so each abutment joint accommodates movement over a temperature range of −10 °F to 110 °F, resulting in a theoretical movement of each joint of approximately 1.3 inches as per AASHTO (2012) specifications. The speed limit on the bridge is 25 miles per hour. The previous joint on this bridge consisted of a poured silicone seal which showed signs of failure, as there was noticeable leaking of water onto the abutment and several rips and punctures throughout the length of the joint. The maintenance crew reported that the seal was installed approximately four years prior to the installation of the foam sealant. Therefore, this bridge allowed for a straight forward comparison of the in-service lifespan of the solid and foam sealant.

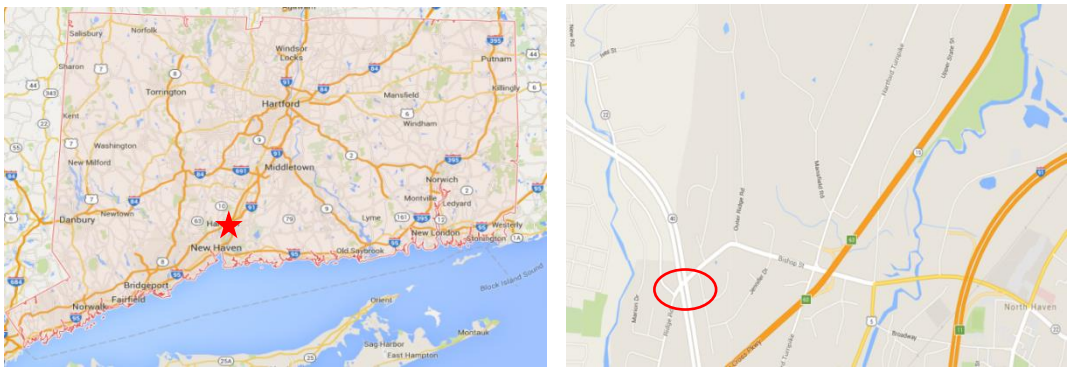

Figure 57: Map location of Route 22 Bridge in North Haven, CT

For this bridge, both joints were sealed for the full width of the bridge deck. This amounted to a total of 80 feet (approximately 40 feet per joint). At the time of installation, the west joint had an average gap opening of 1.00 inches, and the east joint had an average gap opening of 2.00 inches. The east joint had significant imperfections along the length of the joint which varied the gap width by ± 0.50 inches. The installation of the expansion joints of the Route 22 bridge was a one-day operation, conducted on Tuesday, October 20, 2015. Weather conditions for that day were mostly sunny with an average temperature of 58 °F. Roadway temperatures and humidity ranged from 57.2-84 °F and 28-42%, respectively. The entire bridge was sealed in approximately 4.5 hours with minimal traffic disruption.

Similar to the installation procedure of the previous two bridges, the existing expansion joint (also a poured silicone seal) was removed first, and the header of the deck was cleaned using a blade saw to remove any remnants of the old joint and expose a fresh surface of concrete. After this, the entire joint was blown with compressed air to remove

any dust or loose particles from the header. This procedure ensured the best quality header since the blade saw exposed a brand new surface of concrete. The preparation of the joint is shown in Figure 58.

(a) (b)

Figure 58: Joint on Route 22 Bridge: (a) air blasting the joint and (b) cutting of the header surface

Upon cleaning of the joint, a three-inch backer rod was inserted into the west joint along the length of the entire south shoulder and lane 1. The backer rod was inserted approximately one inch below the surface of the roadway. A recess tool was used to push the backer rod to the desired depth to ensure even placement along the entire joint. Once the backer rod was in place, primer was applied at the appropriate locations, as shown in Figure 59. Stoppers were inserted in between areas where the solid sealant was terminated and the foam sealant was poured. Each sealant was poured so that, when a vehicle drove over the joint, one tire hit the solid sealant and the other tire hit the foam sealant. However, this was not always the case due to the Latin square rotation, since the foam sealant could have been located on the west joint and the solid sealant on the east joint.

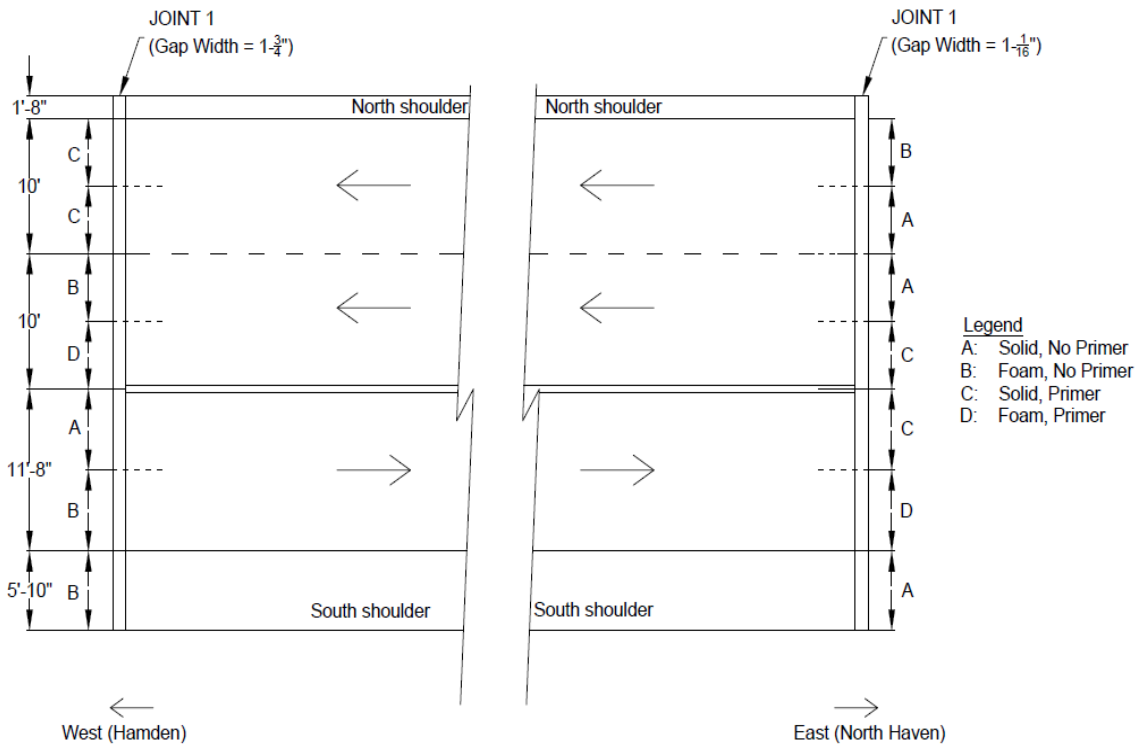

Figure 59: Sealant and primer placement plan, Route 22 Bridge

4.0 FIELD MONITORING

This section outlines the measures taken to monitor the conditions of each bridge onto which the expansion joints were installed. Due to limitations such as seasonal weather, availability of crews, access to substructure, time window for work, and traffic conditions, each bridge was monitored using varying techniques.

4.1 Route 6 Bridge

The Route 6 bridge in Windham, CT, was monitored with the most intensity due to its proximity to UConn, easy access to the substructure, and good relationship with the local maintenance crews. After installation of the sealant, several joint gap readings were recorded on a monthly basis. Additionally, CT DOT generously provided maintenance crews and equipment to assist with the installation of displacement measuring devices onto the east abutment. Through the efforts of the Connecticut Transportation Institute (CTI) and UConn, a traffic counter was installed to conduct continuous monitoring of the vehicles passing over the bridge. Finally, weather data (temperatures, humidity and precipitation) were recorded to examine the nature's effect on the joint gap.

4.1.1 Joint Gap History

Upon installation, the joint gap was measured at several locations along the joint. Since portions of the road were closed during the installation process, a detailed record of the joint gap widths was recorded. However, after installation of the joint, the gaps were measured at limited locations as moving traffic prevented measuring the joint gap due to safety precautions. During installation on Friday, August 14, 2015, the average joint gap for the west joint was 1.625 inches for the west joint and 2.00 inches for the east joint, with an average temperature of 82 °F. On Monday, September 14, 2015, the average joint gap for the west joint increased to approximately 1.685 inches. The east gap that day measured 2.0625 inches. These measurements were recorded at a temperature of 76 °F. On Tuesday, January 12, 2016, the west joint gap measured about 2.0625 inches while the east joint gap measured 2.25 inches at a corresponding temperature of 29 °F. This large shift in joint gap corresponds to a 52 °F drop in temperature since the day of installation. According to Equation 1, the theoretical change in the joint gap is 0.37 inches, assuming the linear thermal coefficient of expansion (α) is 0.000008 R^{-1}. Field measurements indicate that the joint gap increased by about 0.25 inches, somewhat less than the movement calculated theoretically. This may be due to the condition of the bridge bearings, as significant rust and debris has accumulated near the supports over time. The time history of the joint gap is shown in Figures 60 and 61.

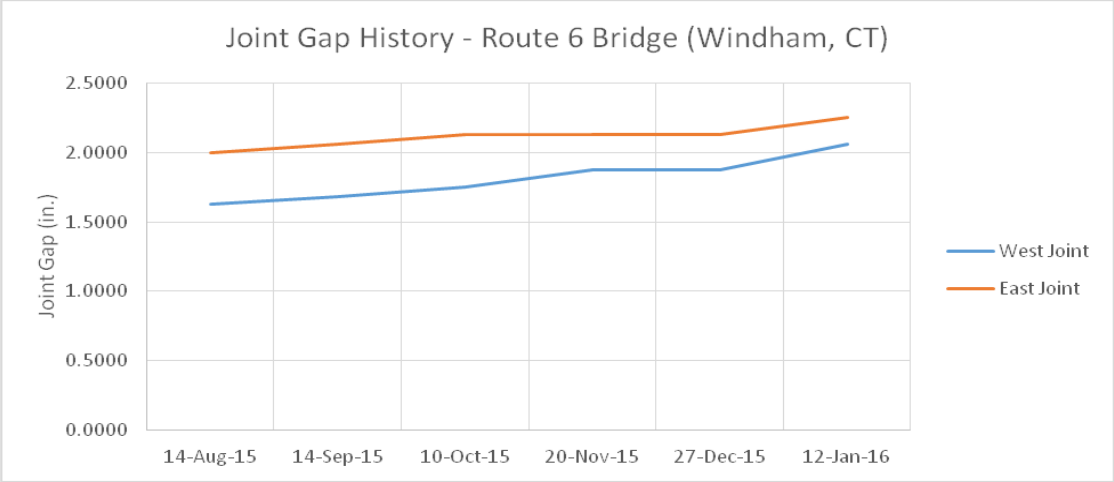

Figure 60: Joint gap history for Route 6 Bridge

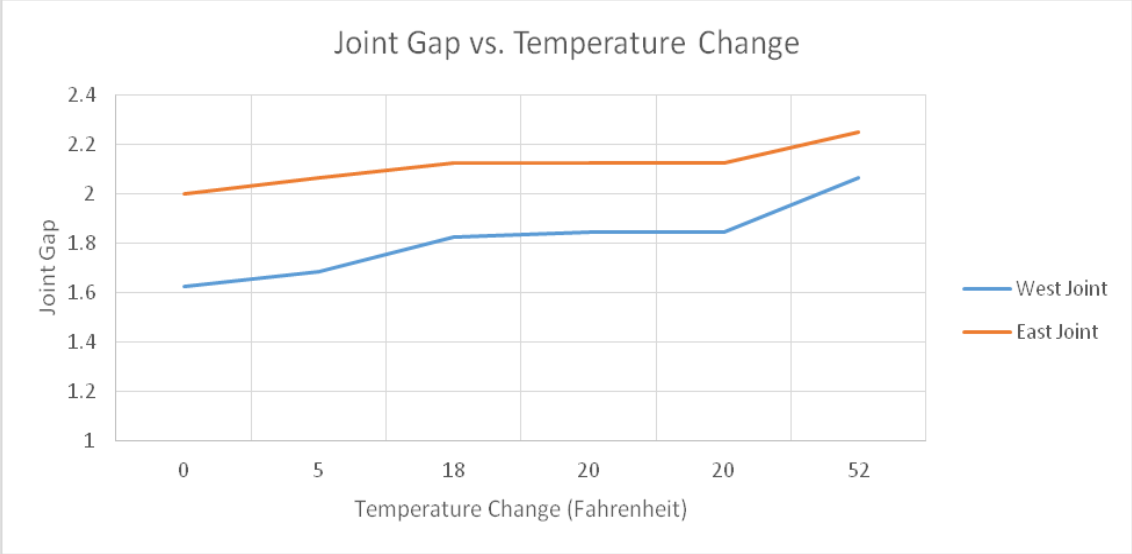

Figure 61: Joint gap as a function of temperature change for Route 6 Bridge

4.1.2 Traffic Counter

Through the assistance of CTI, a traffic counter was installed approximately 100 feet away from the east expansion joint on Route 6 Bridge. The traffic counter could not be installed on the bridge itself because there were no fixtures to secure the computer that recorded and stored the data. However, there are no turns or alternate routes between the bridge and the traffic counter, so the vehicle data was as accurate as possible. The traffic counter consisted of two portable, automatic, pneumatic- tube counters spread across the entire width of the roadway. Tube counters have proven over the years to be inexpensive devices that are fairly easy to install and remove, and that provide adequate accuracy for most applications (Kraft 2008).

The tubes were installed by nailing metal clamps to the asphalt at the outer edges of the roadway. These clamps secured the tubes at each end, while a wire loop held the tube

in place at the median. The wire loop was installed to allow for some movement of the tubes as vehicles drive by; if the tubes were clamped at all three locations, vehicles could rip them off in between the two clamps, but the wire loop provided some flexibility when the vehicles drove over. The west tube was labeled "A" and the east tube was labeled "B". This convention was established to determine the direction of vehicles travelling over the bridge. The tubes were spaced exactly 36 inches apart; this spacing is commonly used when speed data is also desired. An overview of the location of the traffic counter is shown in Figure 62.

Figure 62: Location of traffic counter on Route 6 Bridge

The traffic counter enabled recording of the number, direction, speed, and classification of all vehicles driving over the bridge over a specified period of time. Two 6-day periods were chosen for monitoring. The first period monitored was from 8:23AM on Tuesday, November 24, 2015, to 2:54 PM on Monday, November 30, 2015. This time period, which falls during Thanksgiving, gave a good indication of regular weekday traffic, holiday traffic, and, also, weekend traffic. The second time period monitored was from 9:52 AM on Thursday, December 17, 2015, to 6:48 PM on Wednesday, December 23, 2015. This time period gave a good indication of the traffic flow during a regular week, including a typical weekend.

During the time period from December 17 to December 23, 2015, the bridge experienced approximately 18,000 vehicles per day. The ADT, measured by CT DOT, was approximately 18,600, comparable to the data obtained during the joint gap monitoring process. Figure 63 shows the distribution of vehicle classes that the bridge experienced during that time span. Since this road is not an interstate highway, there are very few trucks or heavy axle load vehicles (vehicles in classes 6-13). The most frequent

vehicle types encountered were those in classes 2 and 3, which are passenger cars and pick-up trucks.

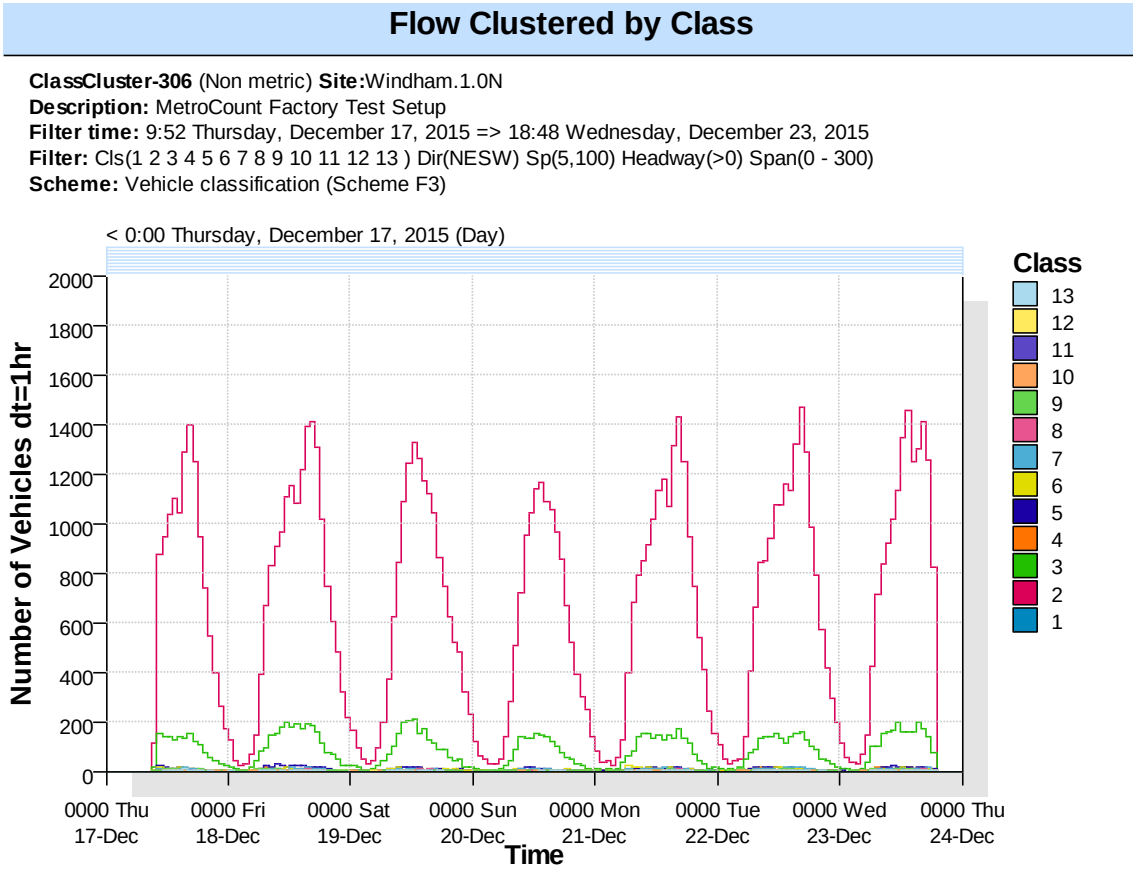

Figure 63: Classification of vehicles entering Route 6 Bridge over monitoring period

Throughout the course of the week from December 17 through December 24, 2015, about 1,400 passenger cars (Class 2 vehicles) drove over the bridge per hour. Class 2 vehicles include all sedans, coupes, and station wagons manufactured primarily for the purpose of carrying passengers, including those passenger cars pulling recreational or other light trailers (FHWA 2014). Class 2 vehicles accounted for 85.3% of the total volume of traffic that the bridge experienced. The second highest class observed was Class 3, which includes all two-axle, four-tire vehicles, other than passenger cars. Since this route accommodates bus traffic, about 0.4% of the volume accounted for passenger-carrying buses with two axles and six tires, or three or more axles. This route experienced truck traffic as well, which included Classes 5-10. Classes 11, 12 and 13 were rarely experienced, as these include multi trailer trucks. Motorcycles accounted for 0.1% of the total traffic volume (total of 142 motorcycles throughout the monitored period). The class and speed distribution is shown in Figure 64.

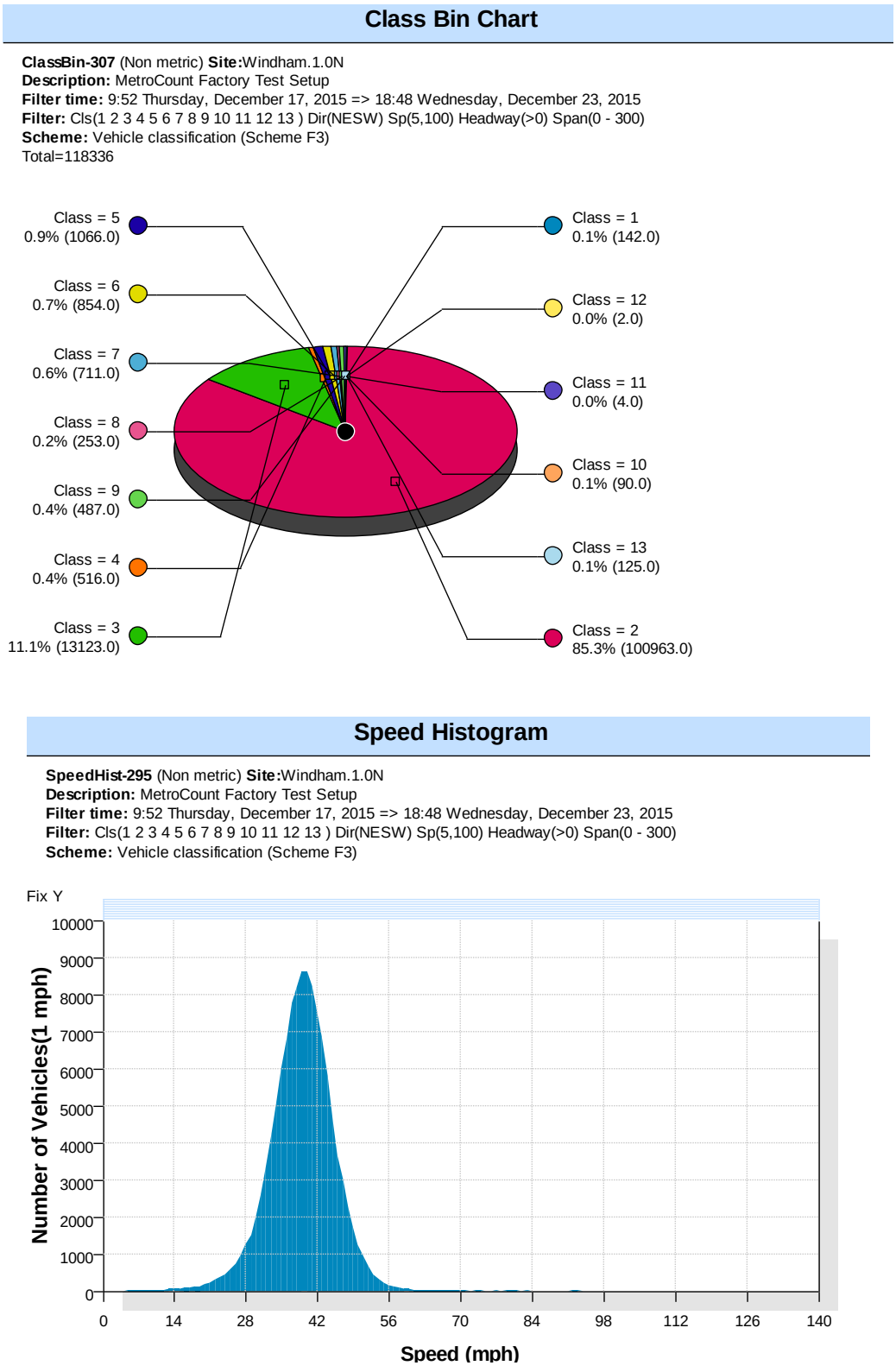

Figure 64: Average speed record for Route 6 Bridge: class bin chart (top) and speed histogram (bottom)

The next measure taken to monitor the Route 6 bridge was to record the axial displacement of the bridge as a function of vehicular movement. In order to do this, several Linear Variable Differential Transformers (LVDTs) were installed onto the girders of the bridge. The devices, supplied by TransTek (2016), have a working range of ± 2 inches with an internal carrier frequency of 1500 Hz. The LVDTs were wrapped with plastic sheeting and duct tape to prevent any moisture from damaging the internal structure of the device. The distance between the end of the girder and the abutment was approximately 16 inches; therefore, the LVDT, alone, could not reach out to make contact with the abutment. In order to attach the devices to the girder and, also, rest the needle onto the abutment, a wooden angle support was constructed and clamped to the girder in such a way so that support extended to the right length. Since the LVDT devices are spring-loaded, they were mounted onto the girders with the needle placed against the abutment (Figure 65). The joints on this bridge are skewed (42 degrees for the west joint, and 45 degrees for the east joint). To prevent the needle from slipping off the abutment, a small hole was drilled into the abutment into which the needle was placed to ensure a proper mounting location. One LVDT was attached onto a girder at two different locations along the east joint. LVDT #1 was attached onto Girder 3, and LVDT #2 was attached onto Girder 6. This placement was designed to gather displacement data at symmetric locations from the edge of the deck, and, also, to monitor the activity at the center of the east and westbound lanes.

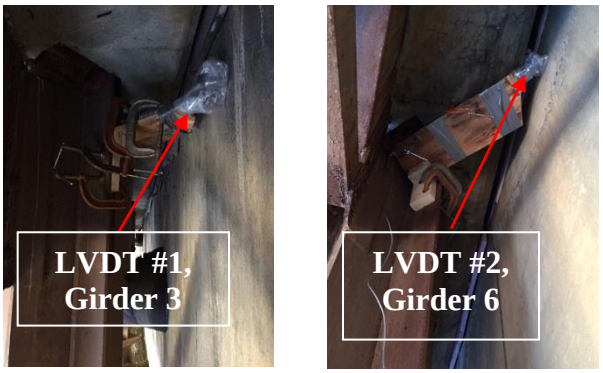

Figure 65: LVDT placement for axial displacement measurement on Route 6 Bridge

The devices were wired to a data acquisition system which recorded the output in the form of voltages. Prior to acquisition, the devices were calibrated in the laboratory to ensure that the displacement readings were accurate and reliable. A sample joint gap movement as a function of vehicular traffic is shown in Figure 66, with the corresponding traffic shown in Table 8.

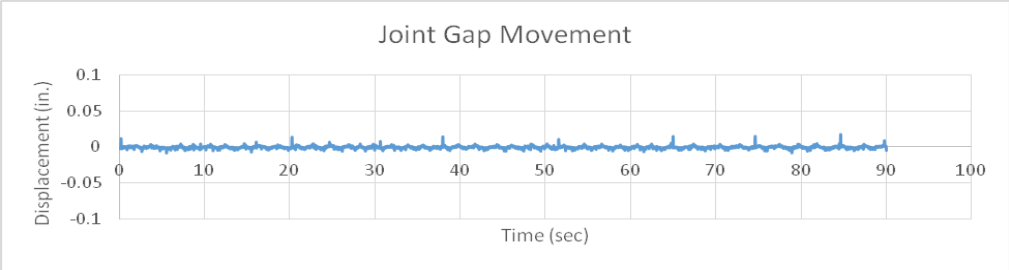

Figure 66: Joint gap movement record of Route 6 Bridge (Windham, CT)

Table 8. Sample vehicle count output on Route 6 Bridge

Count ID	Date	Time	Direction	Speed, mph	Headway, s	FHWA Class
00012bde	12/18/15	9:52:22	N1	42.98	1.7	2
00012be2	12/18/15	9:52:30	N1	38.95	7.6	2
00012be6	12/18/15	9:52:31	N1	38.14	1.3	2
00012bea	12/18/15	9:52:34	N1	36.1	2.7	2
00012bee	12/18/15	9:52:38	S0	44.44	26.3	2
00012bee	12/18/15	9:52:38	S0	44.44	0	2
00012bf5	12/18/15	9:52:40	S0	45.39	1.6	2
00012bf9	12/18/15	9:52:41	N1	39.23	6.9	2
00012bfd	12/18/15	9:52:41	N1	32.27	0.4	2
00012c01	12/18/15	9:52:42	S0	41.1	2.4	3
00012c05	12/18/15	9:52:43	N1	31.2	1.4	2
00012c09	12/18/15	9:52:44	N1	31.71	1.2	2
00012c0d	12/18/15	9:52:52	N1	54.15	7.8	2
00012c11	12/18/15	9:52:52	N1	50.41	0.7	2
00012c15	12/18/15	9:52:55	S0	47.98	13.1	2
00012c19	12/18/15	9:52:56	N1	49.32	3.3	3
00012c1d	12/18/15	9:52:56	N1	46.05	0.4	3
00012c21	12/18/15	9:52:59	N1	44.96	2.9	2
00012c25	12/18/15	9:53:00	N1	43.77	1.4	2
00012c29	12/18/15	9:53:02	N1	37.66	1.6	2
00012c2d	12/18/15	9:53:02	N1	50.73	0.4	2
00012c31	12/18/15	9:53:04	N1	42.13	1.2	2
00012c35	12/18/15	9:53:04	S0	41.13	8.5	2
00012c39	12/18/15	9:53:05	N1	48.45	0.9	2
00012c3d	12/18/15	9:53:08	S0	39.92	3.6	2
00012c41	12/18/15	9:53:12	N1	39.02	7.1	2
00012c45	12/18/15	9:53:15	N1	41.33	3.1	2
00012c49	12/18/15	9:53:16	S0	46.79	8.1	2
00012c4d	12/18/15	9:53:29	N1	44.23	14.6	2
00012c51	12/18/15	9:53:31	N1	39.24	1.9	7

4.2 Route 291 Bridge

The Route 291 bridge was monitored routinely for its joint gap opening as a function of thermal contraction and expansion, and, also, as a function of vehicular movement. Weather conditions such as temperature, precipitation, and humidity were also recorded. However, due to the speed limit and high-priority route, CT DOT did not support installing a traffic counter on the roadway. Therefore, exact traffic data regarding classifications and daily vehicle totals were not obtained.

4.2.1 Joint Gap History

Upon installation, the joint gap was measured at several locations along the joint. Because portions of the road were closed during the installation process, a detailed record of the joint gap widths could be recorded. After the installation of the expansion joint, however, readings were only obtained from the shoulder because of the high speed of traffic and danger associated with measuring the gap at the center of the lanes. During installation on October 6, 2015, the joint gap measured approximately 3.125 inches for the east joint and 3.625 inches for the west joint with an average temperature of 72 °F. On October 17, 2015, the joint gap was measured at 3.25 inches for the east joint and 3.75 inches for the west joint at a temperature of 55 °F. On Wednesday, November 25, 2015, the joint gap measured about 3.375 inches for the east joint. The west joint measured 3.875 inches that day. The corresponding temperature was 48 °F. By January 12, 2016, the temperature dropped to 29 °F; consequently, the joint gap increased to 3.875 inches for the east joint and 4.25 inches for the west joint. This large shift in joint gap corresponds to a 43 °F drop in temperature since the day of installation. According to Equation 1, the theoretical change in the joint gap is 0.7 inches assuming the thermal coefficient of expansion (α) is 0.000008 1/R. Field measurements indicate that the joint gap increased by about 0.875 inches, which is more than the theoretically calculated value. The time history of the joint gap is shown in Figures 67 and 68.

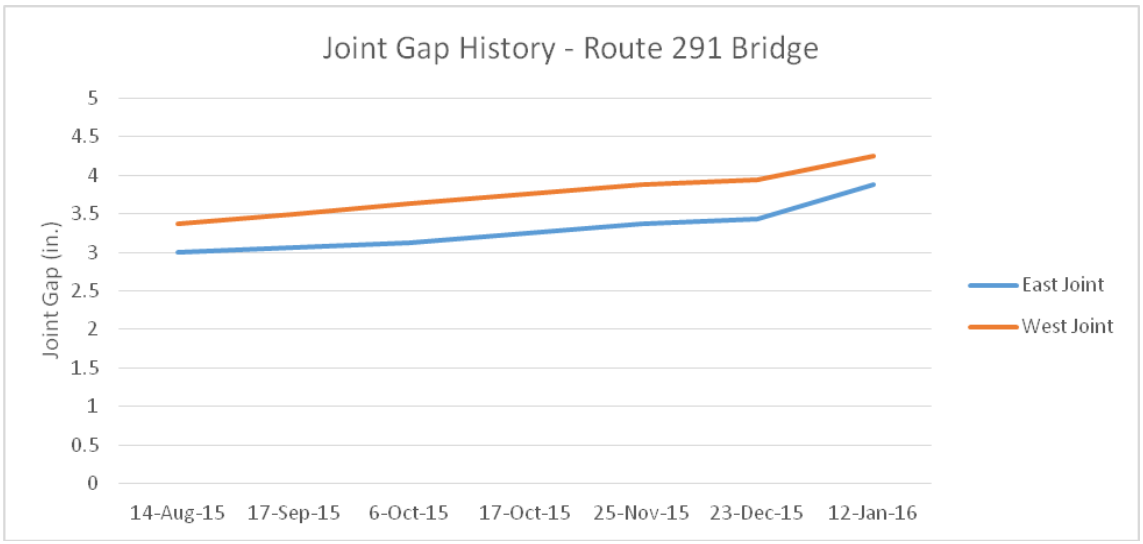

Figure 67: Joint gap history for Route 291 Bridge

4.3 Route 22 Bridge

The Route 22 Bridge was also monitored routinely for its joint gap opening as a function of thermal contraction and expansion. Traffic data and joint gap movement, as a function of vehicular loading, were not obtained for this bridge. The gap opening and the condition of the joint was regularly checked to observe premature or unexpected failing.

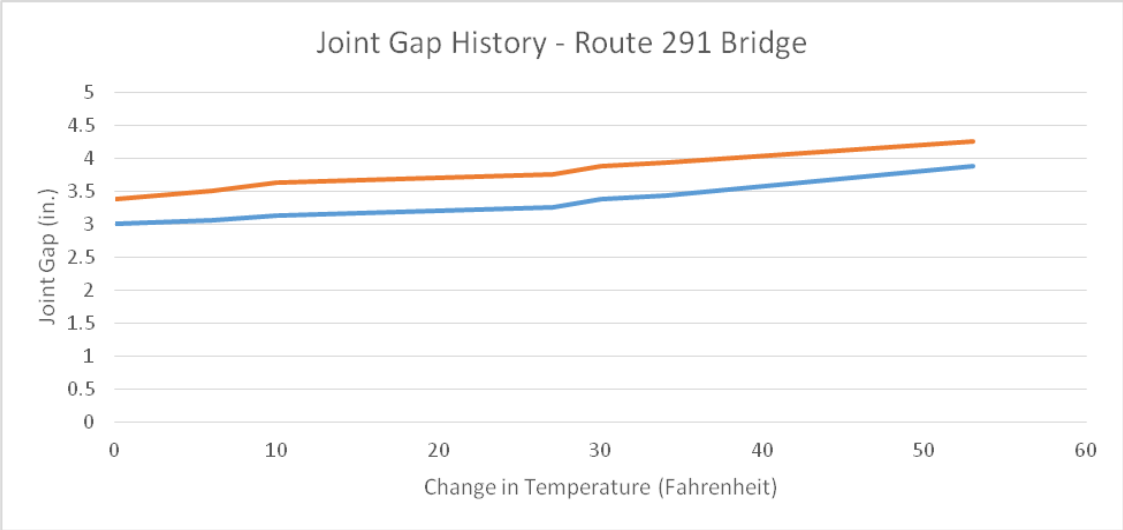

Figure 68: Joint gap vs. change in temperature for Route 291 Bridge

Weather conditions such as temperature, precipitation, and humidity were also recorded. However, due to the speed limit and high priority route, CT DOT did not support installing a traffic counter on the roadway. Therefore, exact traffic data regarding classifications and daily vehicle totals were not obtained.

4.3.1 Joint Gap History

Upon installation, the joint gap was measured at several locations along the joint. Because portions of the road were closed during the installation process, a detailed record of the joint gap widths was recorded. After the installation of the expansion joint, however, readings were only obtained from the shoulder because of the high speed of traffic and danger associated with measuring the gap at the center of the lanes. During installation on October 6, 2015, the joint gap measured approximately 3.125 inches for the east joint and 3.625 inches for the west joint, with an average temperature of 72 °F. On October 17, 2015, the joint gap was measured at 3.25 inches for the east joint and 3.75 inches for the west joint, at a temperature of 55 °F. On Wednesday, November 25, 2015, the joint gap measured about 3.375 inches for the east joint. The west joint measured 3.875 inches that day. The corresponding temperature was 48 °F. By January 12, 2016, the temperature dropped to 29 °F; consequently, the joint gap increased to 3.875 inches for the east joint and 4.25 inches for the west joint. This large shift in joint gap corresponds to a 43 °F drop in temperature since the day of installation. According to Equation 1, the theoretical change in the joint gap is 0.7 inches, assuming the thermal coefficient of expansion (α) is 0.000008 1/R. Field measurements indicate that the joint gap increased by about 0.875 inches, which is more than the theoretically calculated value. The time history of the joint gap is shown in Figure 69.

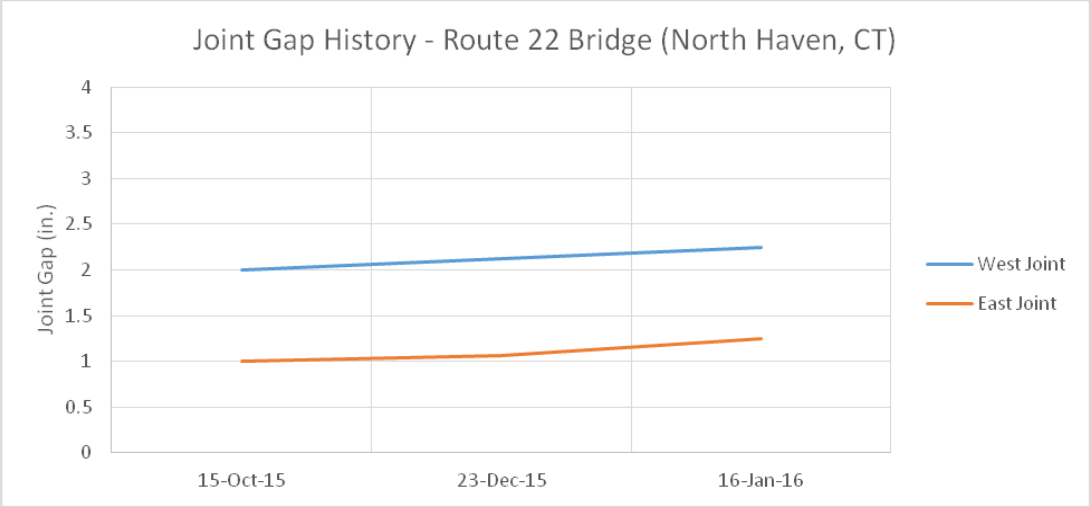

Figure 69: Joint gap history of the Route 22 Bridge (North Haven, CT)

4.4 Visual Inspection of Sealants

Site visits were conducted on each bridge on October 17, 2015; November 25, 2015; January 12, 2016; and, March 23, 2016, for visual inspection. Each visual observation consisted of checking the quality of the sealant itself and observing for any punctures, tears, detachments, or other damage that may compromise the seal of the joint. Photos were also taken to determine common locations of debris build-up. Finally, joint gap-width measurements were taken to record change throughout the season. No damage to the joint or the substrate was observed during the site visits conducted on October 17, 2015; November 25, 2015; and, January 12, 2016.

The first signs of deterioration and/or failure were observed on March 23, 2016, when all three bridge joints were visually inspected. At the time of the visit to the Route 6 bridge in Windham, CT (Bridge No. 2570), on March 23, 2016, the temperature was 51° F, with a humidity of 34%. The east and west joint gaps measured at 2.00 and 2.125 inches, respectively. No damage to the joint or the substrate was observed on this date. There was an accumulation of road salt and other road debris inside of the joint. The accumulation was more significant closer to the shoulder, and in the shoulder itself.

At the time of the visit on March 23, 2016, to the Route I-291 Bridge in Windsor, CT (Bridge no. 06226), the temperature was 53° F, with a humidity of 31%. The east and west joint gaps measured at 3.3125 and 3.9375 inches, respectively. Damage was observed on both joints. Two ruptures (A and B) were observed on the west joint, and one rupture (C) was observed on the east joint (shown in Figures 70-71). Rupture A was observed in the location where solid sealant was applied without primer. Rupture B was observed in the location where foam sealant was applied without primer. Finally, rupture C was observed in the location where foam sealant was applied with primer. All three ruptures were located at the same location along each joint (i.e., right side of the lane, close to the shoulder). Road salt was also accumulating inside the joint, especially towards the shoulder area.

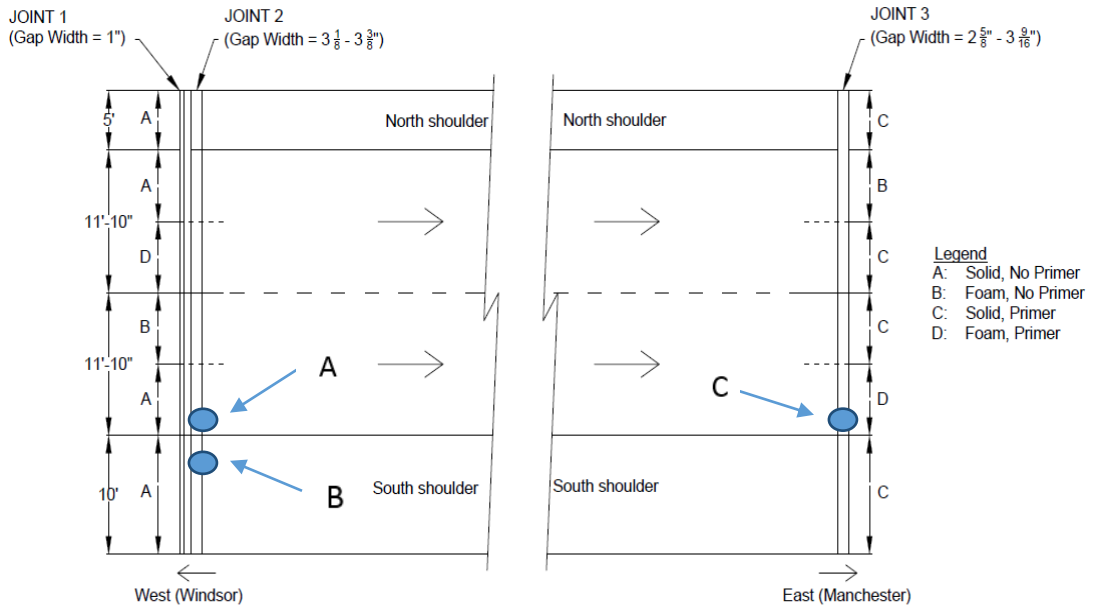

Figure 70: Location of damage on Route 291 Bridge

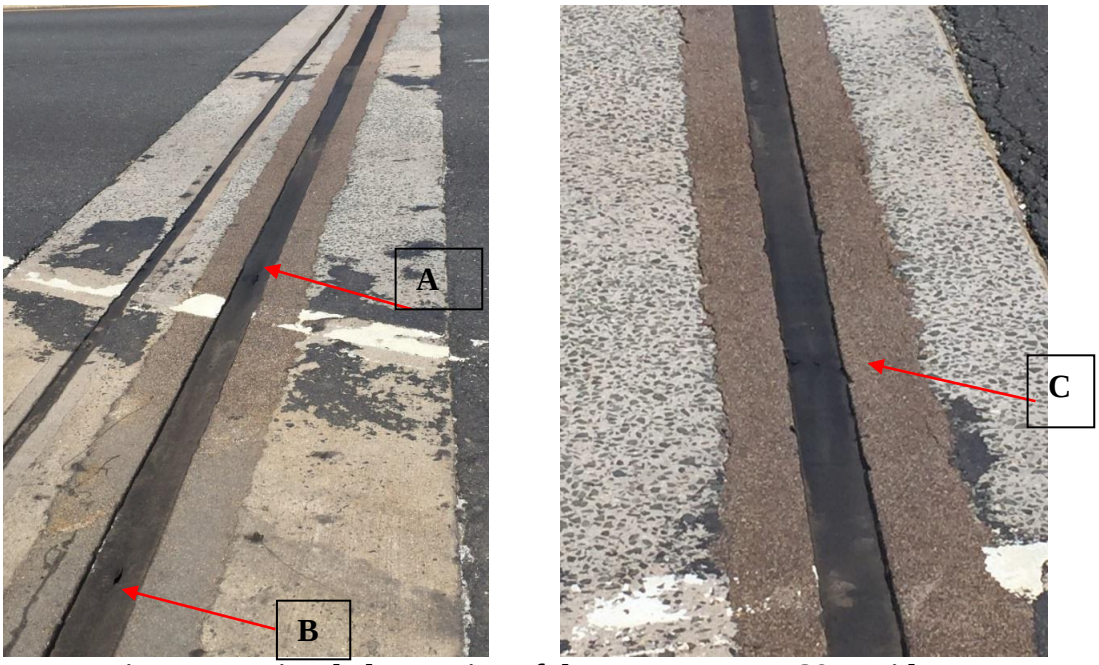

Figure 71: Visual observation of damage on Route 291 Bridge

At the time of the visit on March 23, 2016, to the Route 22 Bridge in North Haven, CT (Bridge No. 03830), the temperature was 54° F, with a humidity of 31%. The east and west joint gaps measured at 1.00 and 2.125 inches, respectively. No damage to the joint or the substrate was observed on this date. Accumulation of debris and some road salt was present, especially towards the shoulder area.

5.0 SUMMARY, CONCLUSIONS AND RECOMMENDATION FOR FUTURE WORK

A silicone foam sealant was developed by modifying a commercially available sealant (termed herein as "solid sealant") and tested in the laboratory to gain a better understanding of the adhesion and bonding characteristics when compared to the solid sealant. Adhesion and tensile characteristics were evaluated by pulling the specimens to failure. Expansion properties were characterized by observing expansion of various initial thicknesses of sealant. Additionally, accelerated laboratory aging of both sealants under the treatment of road salt was conducted to determine the degradation of the bond and modulus between the sealant and the substrate. Finally, the foam and solid sealants were installed on seven joints on three bridges of varying traffic volume, joint gap widths, and joint gap movements to compare the behavior of both sealants under a realistic operating environment with, and without, the application of primer on the header. From these studies, the following conclusions were made:

- Under a tensile load, the foam sealant exhibited a lower modulus (i.e., stress at 100% strain) and a lower ultimate stress. This indicates a smaller stress being developed at the interface of the sealant and the header. This characteristic is favorable when aiming to improve the adhesion properties of poured silicone joints, as the most common mode of failure of the joint is detachment of the sealant material from substrate (material failure was much less common).

- The application of primer onto the specimens yielded no significant difference in tensile and adhesion performance. Although two out of ten specimens containing solid sealant failed via cohesive failure under the influence of primer, it could not be said that primer significantly improves the bonding, as the ultimate elongation was comparable to the specimens with no primer. The foam sealant showed no change in performance, as all specimens failed cohesively.

- The expansion of the foam sealant varies depending on the initial thickness of the sealant applied. When applying a thick coating of 1″, the foam sealant expanded nearly 75%; meanwhile, a coating of 0.25″ produced a total expansion of approximately 50%, for a final thickness of 0.375″. This may be attributed to the volume of additives in the foam sealant, as smaller quantities of foam sealant will contain less crosslinker. The hydrogen gas may tend to escape from the sealant as a whole, instead of creating bubbles within the bulk sealant. For sealants with a larger thickness, however, more time may be needed for the gas to diffuse from the sealant; this may result in an increased foaming effect as more bubbles may stay trapped inside the structure of the sealant.

- The stress at 100% strain (modulus) was observed to drop significantly for the solid sealant over an aging period of six months. The rate of deterioration of the solid sealant was more significant than that of the foam sealant. The specimens treated with primer did not show any noticeable change in modulus as a function of aging. Soaking in road-salt solution did not have a significant effect in the reduction of the modulus of either sealants

- The sealants were installed onto three bridges, at three different locations in the state of Connecticut, to monitor their in-service performance under realistic environmental and vehicular demands. After several site visits, no damage was observed on the Route 6 and Route 22 bridges. However, some punctures and tears were observed on the Route 291 (a bridge that experiences higher traffic volumes and joint gap movements) during the most recent site visit on March 23, 2016.

Based on the research study performed in this project, the following directions can be considered for future work:

- Further development of an applicator that will make field installation easier and more efficient, as combining five ingredients (especially the small amounts of chemical additives) can be difficult. In this regard, it is imperative to develop a two-component formulation, including variations for cold and hot temperature.

- A fatigue test may be beneficial to understanding the behavior of each type of sealant, when repeated impacts cause the material to slightly expand and contract due to the movement of the bridge deck.

- A larger sample size of bridges for field installation may be helpful to determine whether the sealant can adhere to bridges with different geometries, substrate headers, movement behavior, traffic patterns, and environmental conditions.

- Quantitative, or at least ordinal, scoring of sealant field performance is needed. This might be done by observing the leakage at the abutment during a rain event to determine the condition of the seal.

6.0 REFERENCES

AASHTO (2012). *Maintenance manual for roadways and bridges*, American Assoc. of State Highway and Transportation Officials (AASHTO), Washington, D.C.

ASCE (2013). "Report card for America's infrastructure." Infrastructure Advisory Council, American Society of Civil Engineers (ASCE), Reston, VA.

ASTM (2003). "Standard test method for hot water accelerated aging of glass-fiber reinforced cement-based composites." *ASTM Standard C1560*, ASTM International, West Conshohocken, PA. www.astm.org (Aug. 1, 2015).

ASTM (2000). "Standard method for determining tensile adhesion properties of structural sealants." *ASTM Standard C1135*. ASTM International, West Conshohocken, PA. www.astm.org (Aug. 1, 2015).

ASTM (2009). "Standard guide for use of joint sealants." *ASTM Standard C1193*, ASTM International, West Conshohocken, PA. www.astm.org (Aug. 1, 2015).

BASF/WBA (2015). "Bridge and highway maintenance – expansion joint systems." BASF/Watson Bowman Acme (WBA) Corp., Amherst, NY.

Bramel, B.K., Dolan, C.W., Puckett, J.A., and Ksaibati, K. (2000). "Asphalt plug joints: refined material tests and design guidelines." *Transportation Research Record*, No. 1740, 126-134.

Burke, M.P. (1989). "Bridge deck joints." *NCHRP Synthesis 141*, Transportation Research Board, Washington, D. C.

CT DOT (2001). *Bridge inspection manual version 2.1*, Connecticut Department of Transportation (CT DOT), Newington, CT.

CT DOT (2003). *Bridge design manual - 2003 edition*, Connecticut Department of Transportation (CT DOT), Newington, CT.

CT DOT (2015). "Winter highway maintenance operations: Connecticut." Connecticut Department of Transportation (CT DOT), Newington, CT/ Connecticut Academy of Science and Engineering, Rocky Hill, CT.

Dow Corning (2004a). "Dow Corning 902 RCS joint sealant." *Form No. 62-181F-01*, Dow Corning Corporation, Midland, MI. www.dowcorning.com (Nov. 1, 2014).

Dow Corning (2004b). "Dow Corning 1200 OS primer clear." Dow Corning Corporation, Midland, MI. http://www.dowcorning.com/applications/search/default.aspx?R=939EN(Nov.1, 2014).

Dow Corning (2004c). "Dow Corning Construction – Primer P." Dow Corning Corporation, Midland, MI. http://www.bondedmaterials.net/assets/data/dow_corning_primer_p.pdf (Nov. 1, 2014).

Dornsife, R.J. (2000). "Chapter 25: Expansion joints." *Bridge engineering handbook* (W. F. Chen and L. Duan, eds.), CRC, Boca Raton, FL.

DSB (2015). "Expansion joint systems." D.S. Brown (DSB), North Baltimore, OH. http://www.dsbrown.com/Resources/Bridges/Expansion-Joint-Systems-Brochure.pdf (Nov. 1, 2015).

FHWA (1980). "Expansion devices for bridges." *Technical Advisory T5140.15,* U.S. Dept. of Transportation, Washington, D.C.

FHWA (2014). *Traffic monitoring guide,* Federal Highway Administration (FHWA), U.S. Dept. of Transportation, Washington, D.C.

Fincher, H.E. (1983). "Evaluation of rubber expansion joints for bridges." *Rep. No. FHWA/IN/RTC-83/1*, FHWA, U.S. Dept. of Transportation, Washington, D.C., 15–16.

Gelest (2003). "Adhesives and sealants." Gelest Inc., Morrisville, PA. http://www.gelest.com (Nov. 1, 2014).

Hamilton, C. D. (1985). "Bridge deck expansion joints final report." *Rep. No. FHWA-ME-TP-84-04*, Maine Department of Transportation, Augusta, ME.

IL DOT (2011). "Silicone bridge joint sealer." *Manuals, Guides and Handbooks*, Illinois Department of Transportation, IL.

Instron 1011 (2010). "Instru-Met remanufactured Instron model 1000 series test frames." Instru-Met Corporation, Union, NJ, USA. (Nov. 1, 2014).

Kraft, W.H., Ed. (2008). "Traffic engineering handbook." *Publication No. TB-010B.* Institute of Transportation Engineers, Washington, D.C.

Kruszewski (2016). "Salt-water aging, bonding, and in-Service performance of a novel poured silicone expansion joint sealant for small movement bridges." *M. S. Thesis* (Faculty Advisor: R. Malla), Univ. of Conn., Storrs, CT.

Lee, D.J. (1994). *Bridge bearings and expansion joint,* Alden Press, Oxford, UK.

Lesa Systems (2016). "Lesa G joint system." Lesa Systems Ltd., Auckland, New Zealand.

Lourakis, M.I.A. (2005). "A brief description of the Levenberg-Marquardt algorithm implemented by Levmar." Institute of Computer Science, Crete, Greece.

http://users.ics.forth.gr/~lourakis/levmar/levmar.pdf (Dec. 15, 2015).

Malla, R., Shrestha, M., Shaw, M., and Boob, S. (2005a). "Silicone foam sealant for bridge expansion joints," *Proc*., 2005 Joint ASCE/ASME/SES Conference on Mechanics and Materials - McMat 2005; Baton Rouge, LA, June, 6 pages.

Malla, R., Shrestha, M., Shaw, M., and Boob, S. (2005b). "Experimental evaluation of silicone foam sealant for bridge expansion joints." *Paper #416, Proc.,* 2005 SEM Annual Conf. and Expo., Soc. for Experimental Mech. (SEM), Bethel, CT, 8 pages.

Malla, R., Shaw, M., Shrestha, M., and Boob, S. (2006). "Sealing small movement bridge expansion joints*." NETCR-58, Final NETC 02-6 Project Rep*., New England Transportation Consortium, Fall River, MA, June, 112 pages. http://www.uvm.edu/~transctr/pdf/netc/netcr58_02-6.pdf.

Malla, R.B., Shaw, M.T., Shrestha, M.R., and Brijmohan, S.B. (2007). "Development and laboratory analysis of silicone foam sealant for bridge expansion joints." *J. Bridge Eng*., 12(4), 438–448.

Malla, R.B., Swanson, B., and Shaw, M.T. (2011a), "Laboratory evaluation of a silicone foam sealant for field application on bridge expansion joints." *Experimental and Applied Mechanics*, Proc. of the 2010 Conference Society for Experimental Mechanics Series, Vol. 6, Springer Publishing , New York, May, 805-816.

Malla, R.B., Shrestha, M. R., Shaw, M.T., and Brijmohan, S.B. (2011b). "Temperature aging, compression recovery, creep, and weathering of a foam silicone sealant for bridge expansion joints." *J. Mater. Civ. Eng*., 23(3), 287–298.

Malla, R.B., Shaw, M.T., Swanson, B., and Gionet, T. (2011c). "NETC 02-6: Sealing small movement bridge expansion joints (Phase 2) – Field demonstration and monitoring." *Final Project Report, Project NETC 02-6,* New England Transportation Consortium, Fall River, MA, July 31, 2011, 128 pages. http://www.uvm.edu/~transctr/pdf/netc/netcr86_02-6_phase2.pdf (Sept. 15, 2015).

Malla, R.B., Swanson, B., and Shaw, M.T. (2011d). "Laboratory evaluation of a silicone foam sealant bonded to various expansion joint header materials." *Constr. Building Mat*., 25(11), 4132–4143.

Milner, M.H. and Shenton III, H. W. (2014). "Survey of past experience and state-of-the-practice in the design and maintenance of small movement expansion joints in the Northeast." *Report 242,* Transportation System Preservation Technical Services Program (TSP2), Univ. of Delaware, Newark, DE. http://sites.udel.edu/dct/files/2013/10/Report-242-TSP2-Small-Movement-Expansion-Joints-2dzoc1e.pdf (Sept. 01, 2015)

MM Systems (2015). "Waterproof expansion joints." MM Systems Corp., Pendergrass, GA, USA.

PSI (2015). *PSI-Plot*, Poly Software International (PSI), Pearl River, NY, USA.

Purvis, R. (2003). "Bridge deck joint performance." *NCHRP Synthesis 319*, Transportation Research Board, Washington, D.C.

Shrestha, M.R., Malla, R.B., Boob, S. and Shaw, M.T., (2006). "Laboratory evaluation of weathering and freeze-thaw effects on silicone foam bridge joint sealant." Paper #369, *Proc.,* 2006 SEM Annual Conference and Exposition, SEM, Bethel, CT, 8 pages.

Swanson, B.J., Malla, R.B., and Shaw, M.T. (2013). "Laboratory testing, field installation, and monitoring of a silicone foam sealant for bridge expansion joints." *J. Bridge Engineering*, 18(8), Aug., 758-767.

Tensa (2015). "Cantilever finger joints – TENSA-FINGER RSFD." Mageba Ltd, Eastern Creek, Australia. http://www.mageba.com.au.

TransTek (2016). "TransTek series 240 general purpose DC LVDTs." TRANS-TEK, Inc., Ellington, CT. http://transtekinc.com/products/series-350/ (Jan. 2015, 2016).

Tremco (2014). "Sealant restoration guide." *Guide to Commercial Sealants and Waterproofing*, Tremco Waterproofing. Beachwood, OH. http://www.thorosystem.com/Documents/SEALANT_RESTORATION_GUIDE_10-6-08.pdf (Feb. 5, 2016).

USC (2015). "Febajoint highways agency type 2 asphaltic plug joint." Universal Sealants Company, England, U.K.

WBA (2001). "WABO_SiliconeSeal installation procedure." Watson Bowman Acme Corp., Amherst, NY. http://www.wbacorp.com/Products/ProductInstallationProcedures.aspx?ProductlineID=48 (Nov. 1, 2014).

WBA (2008a). "WABO_SiliconeSeal." Watson Bowman Acme Corp., Amherst, NY. https://wbacorp.com/products/bridge-highway/joint-seals/wabo-siliconeseal-bridge/ (Nov. 1, 2014).

WBA (2008b). "Wabocrete II." Watson Bowman Acme Corp., Amherst, NY. https://wbacorp.com/products/parking-sturctures-and-stadiums/accessories-parking-stadiums/wabo-crete-ii/.

WBA (2008c). "WABO_SiliconeSeal installation procedure." Watson Bowman Acme Corp., Amherst, NY. https://wbacorp.com/public/userfiles/WaboSiliconeSeal_Install.pdf (Nov. 1, 2014).